# 1

# Background and Introduction

This chapter provides a background to the common realizations and dynamics of bistable structures which have recently been harnessed to advance the aims of the three technical areas of interest in this book: vibration control, vibration energy harvesting, and sensing and detection. The structural forms and dynamical behaviors of bistable systems are first introduced to demonstrate the broad versatility of design and response which are commonly exploited, and to highlight the dynamics which are enabled via leveraging bistability. Then, two aspects of bistable structural dynamics are identified as trademark features which serve as common rationales for exploiting bistability in engineering applications. These aspects are elaborated upon through concise descriptions of example implementations within the technical areas considered here. Finally, an outline of the remaining chapters is provided.

## 1.1 Examples of Bistable Structures and Systems

To introduce the essential static characteristics of a bistable structure, a schematic of an example one-dimensional, mechanical bistable system is shown in Figure 1.1. To set a clear convention, hereafter the terms bistable *structures* and *systems* will be used interchangeably, irrespective of whether the object considered is all-mechanical, electromechanical, or all-electrical. For the bistable system shown in Figure 1.1, two identical springs of undeformed lengths $l_o$ connect a lumped mass to a surrounding frame of span $2d$. It is assumed that all displacements of the system are in a horizontal direction, such that the frame motions $z$ and mass displacements $X$ move along one axis. When the undeformed spring length is less than or equal to half of the span of the frame, $l_o \leq d$, the system is monostable and the mass will come to rest at the zero displacement position, $X = 0$. In contrast, when the undeformed spring length is greater than half of the span of the frame, $l_o > d$, the springs exert a force on the mass such that the mass cannot be easily maintained in the central configuration. The zero displacement configuration is unstable, while two stable positions of the mass are adjacent (and, here, symmetric) to the central, unstable state. As a result of the geometric design condition $l_o > d$, the mass-spring and frame system is said
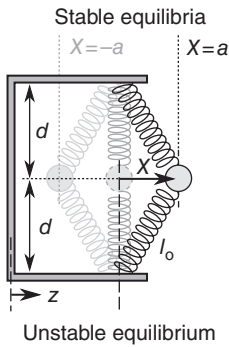
Stable equilibria

$X=-a$     $X=a$

Unstable equilibrium

**Figure 1.1** Schematic of a bistable system composed of springs, mass, and frame. Here $l_o > d$ which makes the central configuration $X = 0$ an unstable position of static equilibrium.

to be *bistable.* The stable equilibria of the structure are shown to be configurations of the mass such that the displacements are $X = \pm a$.

Figure 1.2a,b illustrates the force, $F(X)$, and potential energy, $U(X)$, of the bistable system, respectively, as functions of the mass displacement. Potential energy is determined by $U = \int F \cdot dX$. In this example, the bistable structure is symmetric and the only forces resisting the horizontal mass displacements are due to the identical springs. Figure 1.2a shows that the total restoring force in the $X$-axis is zero when the inertial mass is positioned at any of the equilibria. On the other hand, Figure 1.2b shows that the potential energy is locally maximized at the unstable central configuration of the inertial mass $X = 0$, while the adjacent, stable equilibria at $X = \pm a$ locally minimize the potential energy of the system. Therefore, based on the principle of minimum total potential energy, disturbances to the inertial mass when it is originally positioned at the unstable equilibrium will propel the mass towards one of the stable equilibria.

An instructive analogy is that of a ball on a terrain with elevation profile shaped like the potential energy plot in Figure 1.2b. While situated precisely at the peak of the central hill (at $X = 0$), the ball will remain stationary even though the gravitational potential energy is high. But if given a slight perturbation, the ball will roll into the nearest valley where it settles into the displacement position which minimizes potential energy (specifically, gravitational potential energy in this analogy).

By Hooke's law, the stiffness of a spring element is determined by the spatial derivative of the restoring force, $dF/dX$. Considering the total spring force profile at the unstable equilibrium in Figure 1.2a, it is apparent that the bistable spring is characterized as having a *negative stiffness* for this mass position. In contrast to a spring which *resists* the motion of the mass in a given direction, a spring exhibiting negative stiffness over a range of displacements will *assist* the motion of the mass. As a result, the small perturbation to the inertial mass when precisely positioned at the unstable equilibrium will lead the bistable spring to propel the mass away from the central location to one of the stable system configurations.

All the bistable systems considered in this book share these fundamental, static characteristics illustrated using the mechanical example in Figure 1.1. In fact, the existence of two statically-stable equilibria configurations and one unstable configuration make it straightforward to identify bistable structures or systems. However, the type of geometrical constraints exemplified in the mechanical
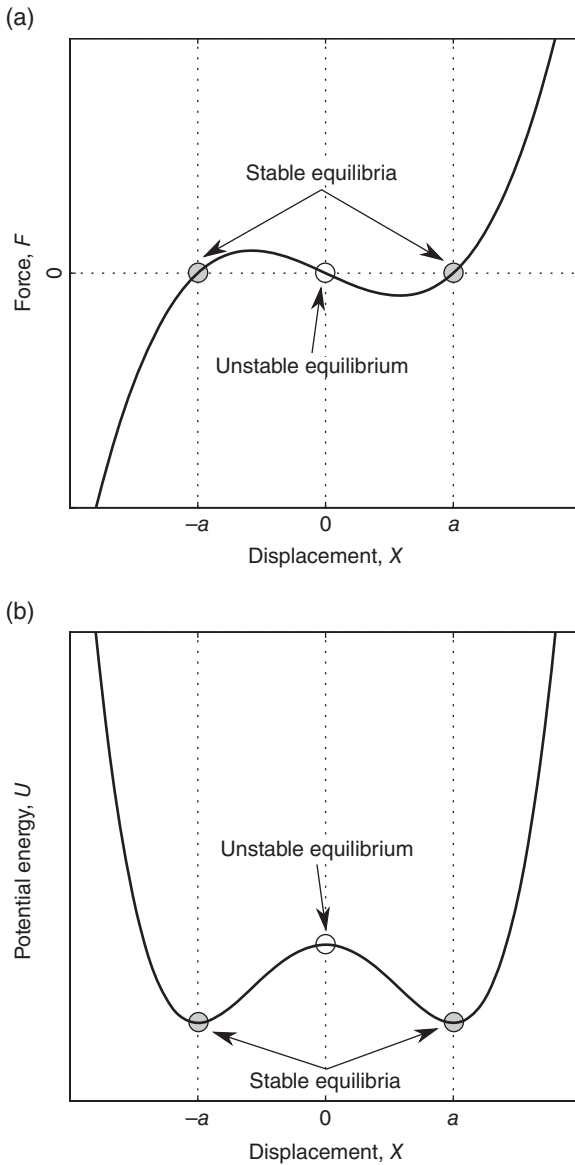
(a)



(b)



**Figure 1.2** Dependence of (a) spring force and (b) stored potential energy on the displacement position of the inertial mass.

device shown in Figure 1.1 are just one possible approach to effect bistability. For the technical areas of vibration control, energy harvesting, or sensing, numerous and diverse methods are employed to realize bistability.
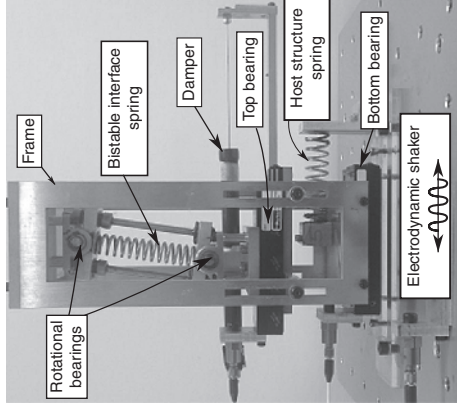
To sample the many approaches, Figure 1.3 shows recently investigated engineering systems that utilize one of the various methods to effect bistability. In Figure 1.3a, modules of series- and parallel-assembled double-beam units are compressed within a housing support near the threshold of buckling. When the
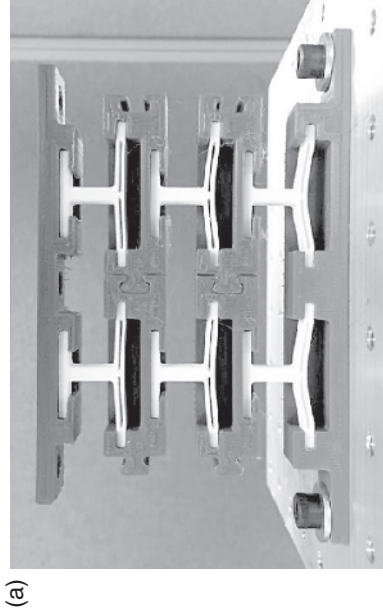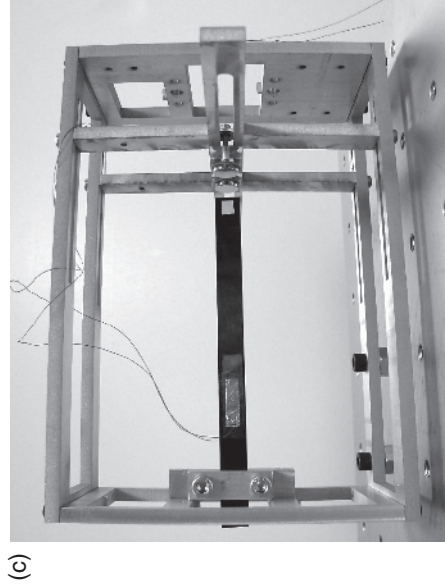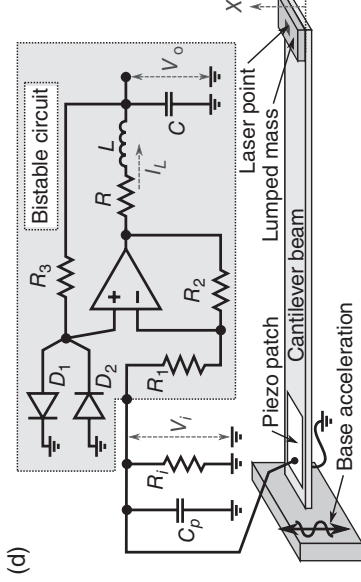
**Figure 1.3** (a) Damping module of buckling beams arranged in series and parallel within a housing frame for energy attenuation between the ends of the module. (b) Bistable device for vibration isolation of suspended top bearing mass. (c) Cantilevered beam with piezoelectric PVDF patches and magnetic attraction induced bistability for energy harvesting. (d) Bistable circuitry attached to host beam structure via piezoelectric transducer for sensing structural change.

statically compressed modular structure is excited with periodic dynamic loads, the modules provide high damping due to the transitions among the various stable topologies. Such transition phenomena result in a large dissipation of the input energy according to the number of state changes that occur. In Figure 1.3b, a two degrees-of-freedom (DOF) vibration suspension concept is shown [1]. Here, bistability is effected between the DOF (the moving frame and top bearing mass) via geometric relations, comparing the length of the interfacing spring to the distance between the frame and top bearing mass. Due to the activation of unique bistable dynamics, the investigations of the two DOF suspension system uncover an exceptional reduction of motion transmissibility as compared to the counterpart two DOF linear suspension [1]. Note that the geometrical constraints in the two DOF architecture shown in Figure 1.3b which lead to bistability between the two moving bodies are similar to those constraints employed in the translational single DOF bistable system example shown in Figure 1.1.

In some vibration energy harvesting applications [2], a composite plate with attached piezoelectric patches is made bistable through the generation of a static stress for the flattened plate configuration, such that the plate maintains one of two stable equilibria shapes having finite curvatures. There are numerous design and fabrication parameters which may be adjusted to tailor the two stable plate curvatures, including the composite material layer selection, lay-up order, layer relative rotations, and thermal conditions under which the layers are stacked and cured [2,3]. When the plate is excited at its center by external vibrations, the energetic snap-through actions of the plate from one stable curvature to the next greatly strain piezoelectric materials attached to the plate surface. In consequence, the input vibrational energy is converted by the piezoelectric material to an oscillating flow of current which can be exploited for energy storage purposes (e.g., battery charging) or conditioned for direct utilization as a supply for low-power microelectronics. In another vibration energy harvesting investigation, bistability is realized using a combination of elastic and magnetic restoring forces on a cantilever beam, as shown in Figure 1.3c [4]. Motions of the ferromagnetic cantilever beam tip are resisted via the beam's inherent elasticity but the attractive influences of the magnet pair are tuned so as to draw the beam away from the original cantilevered configuration. The piezoelectric PVDF (polyvinylidene fluoride) patches attached to the beam surface are significantly strained as ground motions excite the cantilever base and cause the beam to oscillate between the stable beam positions. Similar to the case of the bistable plate, the charge generation on the piezoelectric material electrodes may then be harnessed for energy harvesting purposes. The broad frequency bandwidth and high sensitivity at low frequencies of snap-through dynamics set bistable energy harvesters apart from other harvester platform designs and strongly justify the recent attention given to bistable structures for energy harvesting applications [5,6].

Bistability may also be effected via electromechanical or electrical means. For instance, due to electrostatic actuation including bias and oscillating voltages, a microbeam having an initial curvature may be excited to oscillate between two stable beam shapes [7]. In this example, the beam may or may not be inherently bistable due to elastic influences alone. Nevertheless, the electrostatic forces provide a means to ensure bistability and then to actuate the beam between the

two stable shapes. The applications for micro- and nanoscale bistable systems are numerous, and include their implementation as electromechanical signal filters, switches, actuators, or as novel mechanical memory elements, to name only a few of the functions for which they have been explored [7–10]. Additionally, the circuit schematic shown in Figure 1.3d realizes bistability simply by the circuit design [11]. In the absence of an input voltage $V_i$, the output voltage $V_o$ across the capacitor $C$ will settle on a finite positive or negative value. Bistable circuitry is a well-established tool in the study of many physical sciences [12], but the exploitation of such circuit designs to advance the aims in engineering contexts is an emerging area of technical interest. For example, when the circuit input is connected to a structural transducer, such as a piezoelectric patch as shown in Figure 1.3d, the activation of the high amplitude snap-through response of the bistable circuit output voltage $V_o$ can be harnessed as an indicator of change in the structural system. By this strategy, one may monitor shifts in important parameters, such as a reduction in stiffness which could indicate damage. Thus, small variations in structural responses of the beam are tracked using large changes in bistable circuit voltage dynamics. Through a relation between the changing structural model parameters and the critical conditions that activate the circuit snap-through dynamics, one realizes a novel pathway for robust and sensitive detection of change [11].

As exemplified by the cross-disciplinary sample described above, the bistable systems considered in this book represent diverse mechanical, electromechanical, and electrical platforms that span a vast range of length scales. Yet, regardless of the specific manifestation and inducement of bistability, the existence of two statically-stable configurations and one unstable configuration is the common denominator for all bistable systems. However, the mechanics of bistable structures are historically-established science [13]. Thus, following the previous introduction of the essential static features of bistable systems and how they have been realized in structural or system forms, the next section introduces the numerous, characteristic *dynamics* of bistable structures. These are the behaviors which have been recently harnessed to the advantage of the technical areas of interest in this book.

## 1.2   Characteristics of Bistable Structural Dynamics

Regardless of the method by which bistability is effected, each platform shown in Figure 1.3 exemplifies dynamics common to all bistable systems. Moreover, these dynamics have particularly unique manifestations as compared to the responses exhibited by linear or monostable nonlinear systems, which justifies the recent research attention given to bistable structures in the technical areas of interest in this book. The following sections review the distinct dynamic characteristics of bistable structures and provide illustrative and exemplary plots of the behaviors. Before elaborating on the unique dynamical features, a brief description is provided below regarding the means to model and predict such dynamics and the interpretations of the parameters that have been employed to generate the illustrative results.

   The illustrative plots presented in the following sections are computed as the dynamic solutions to the governing equation of motion of a bistable system. The analytical and numerical techniques to solve the equation, so as to generate the following plots, are described in detail in Chapter 2. A conventional governing equation construction is used which is known to accurately model the dynamics of numerous bistable structure realizations that have been examined across a wide range of sciences and engineering fields. The equation may be expressed in a normalized form as

$$\frac{\mathrm{d}^2 x}{\mathrm{d}\tau^2} + \gamma \frac{\mathrm{d}x}{\mathrm{d}\tau} - x + \beta x^3 = p \cos \omega\tau \tag{1.1}$$

where $x(\tau)$ is considered to be the non-dimensional, generalized displacement of the bistable structural system which is a function of non-dimensional time $\tau$; $\gamma$ is a damping factor; $\beta$ is a degree of nonlinearity; $p$ is the excitation level. The term $\omega$ is the excitation frequency which is normalized according to the system's natural frequency computed using the magnitude of the linear stiffness and the mass of the non-normalized system [14]; thus, $\omega = 1$ indicates a resonance-like excitation, although the analogy is imperfect. The transient solution to Eq. (1.1) also depends on the initial conditions of displacement and velocity, $x(0)=x_0$ and $\dot{x}(0) = \dot{x}_0$, respectively, where an overdot indicates differentiation with respect to the normalized time, $\mathrm{d}/\mathrm{d}\tau$.

   Although the following examples describe the characteristic dynamics computed from Eq. (1.1) in regards to a bistable *mechanical* system response, in which case terms such as displacement and velocity will be used, it is noted for completeness that Eq. (1.1) also models bistable systems realized in electrical domains. Thus, the coordinate $x$ may represent a normalized voltage or current and the corresponding system and excitation parameters $(p,\omega,\gamma,\beta)$ may be described in terms of the appropriate counterpart electrical components.

   The unforced, static solution to Eq. (1.1) leads to the determination of the equilibria configurations of the bistable system. In this case, one solves an equation expressed by

$$-x + \beta x^3 = 0 \tag{1.2}$$

   The solutions to the polynomial in Eq. (1.2) are $x = \pm 1$ and 0. Further mathematical treatment of these results, detailed in Chapter 2, reveals that the equilibria at $x = \pm 1$ are *stable* whereas the equilibrium at $x = 0$ is *unstable*.

   Using the analytically or numerically computed solutions to the governing equation and by taking into consideration the bistable system equilibria configurations, the following sections elaborate on the characteristics of bistable structural dynamics. While some of the general dynamical features are exhibited by other types of nonlinear systems, the unique ways in which they are realized by bistable structures are detailed to highlight the important distinctions. For brevity, the following sections describe and elucidate the plotted results while the figure captions detail the specific parameter set combinations and relevant computational aspects to generate the data.

### 1.2.1 Coexistence of Single-periodic, Steady-state Responses

In contrast to linear systems, when driven by single-frequency excitations many nonlinear systems may potentially exhibit one or more forms of steady-state response that *coexist* as a result of the same excitation conditions. These vibrations occur primarily at the excitation frequency. The coexistence of dynamic responses means that for a set of design parameters and prescribed harmonic excitation level and frequency, the nonlinear system may undergo different dynamics in time, often one of two distinct harmonic response amplitudes. The specific dynamic that occurs is dependent upon the system initial conditions at the starting time of the single-frequency excitation.

In the case of bistable systems, there are numerous types of single-periodic, steady-state dynamics which may coexist. First, one may classify the dynamics into two regimes: *intrawell* oscillations which occur around one of the two stable equilibria, or *interwell* oscillations which vibrate across the unstable equilibrium twice per excitation cycle. Because the potential energy profile of bistable systems, shown in Figure 1.2b, is conventionally referred to as the *double-well* potential, the terms *intrawell* and *interwell* denote that the oscillations of the inertial mass remain confined to one of the local wells of potential energy or cross back-and-forth between them, respectively. One may then separate these two dynamic regimes into low and high amplitude versions of the intra- and interwell dynamics. As a result, there are *four* forms of single-periodic, steady-state dynamics exhibited by a bistable structure, some of that may coexist for the same excitation and system design parameters.

As examples of the two forms of *intrawell* dynamics, Figure 1.4a presents numerically computed displacement responses using Eq. (1.1). Here, the different initial conditions lead to unique steady-state dynamics while all other parameters remain the same. It is clear that the intrawell dynamics, plotted as the black or gray solid curves, oscillate around one of the two stable equilibria shown as thick dotted lines. Although not able to be observed using one example, the low and high amplitude oscillations, as predicted from Eq. (1.1), may occur around either stable equilibrium. In the example presented in Figure 1.4a, the initial conditions are such that the high amplitude oscillations vibrate around the stable equilibrium at $x = -1$ while the low amplitude responses occur around $x = +1$. Figure 1.4b plots the displacement amplitude across all frequencies as a consequence of the excitation at frequency $\omega$. The data are computed using the fast Fourier transform (FFT) of the displacement time series shown in Figure 1.4a; the final 50 of 100 excitation periods are used in the computation. The spectra shown in Figure 1.4b plainly indicate that the different intrawell dynamics are distinct in their amplitude at the excitation frequency, shown as the circle points. The input energy at the frequency of $\omega$ is apparently diffused to other harmonics; further discussion of this feature is deferred until Section 1.2.6.

Figure 1.5a plots an example in which the low and high amplitude *interwell* dynamics are found to coexist for the same excitation frequency and level. The interwell behaviors are distinct from the intrawell responses in that the prior oscillate across the unstable equilibrium position, which was identified above to be the normalized position of $x = 0$. Apart from the difference in the amplitudes
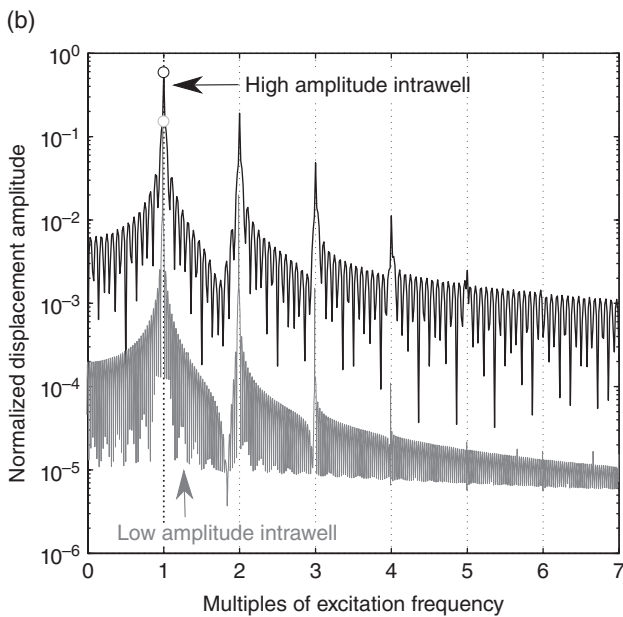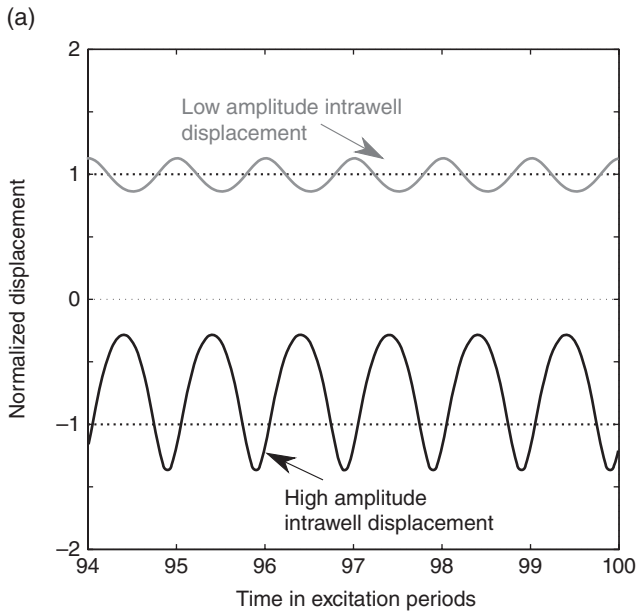
(a)



(b)



**Figure 1.4** (a) For an excitation frequency at which both the low and high intrawell dynamics coexist, the time series of the displacement responses are presented. The thick dotted lines indicate the statically-stable equilibria. (b) The displacement magnitude spectral responses of the low and high amplitude intrawell dynamics are shown as computed from the time series data plotted in (a). The energy diffusion to other harmonics of the excitation frequency is apparent and distinct between the response forms. In (a,b), the parameters are $(p, \omega, \gamma, \beta) = (0.1, 1.1, 0.09, 1)$, with initial conditions $(x_0, \dot{x}_0) = (1.0041, 0.0961)$ for the low amplitude oscillations and $(2.2858, -0.9302)$ for the high amplitude dynamics.
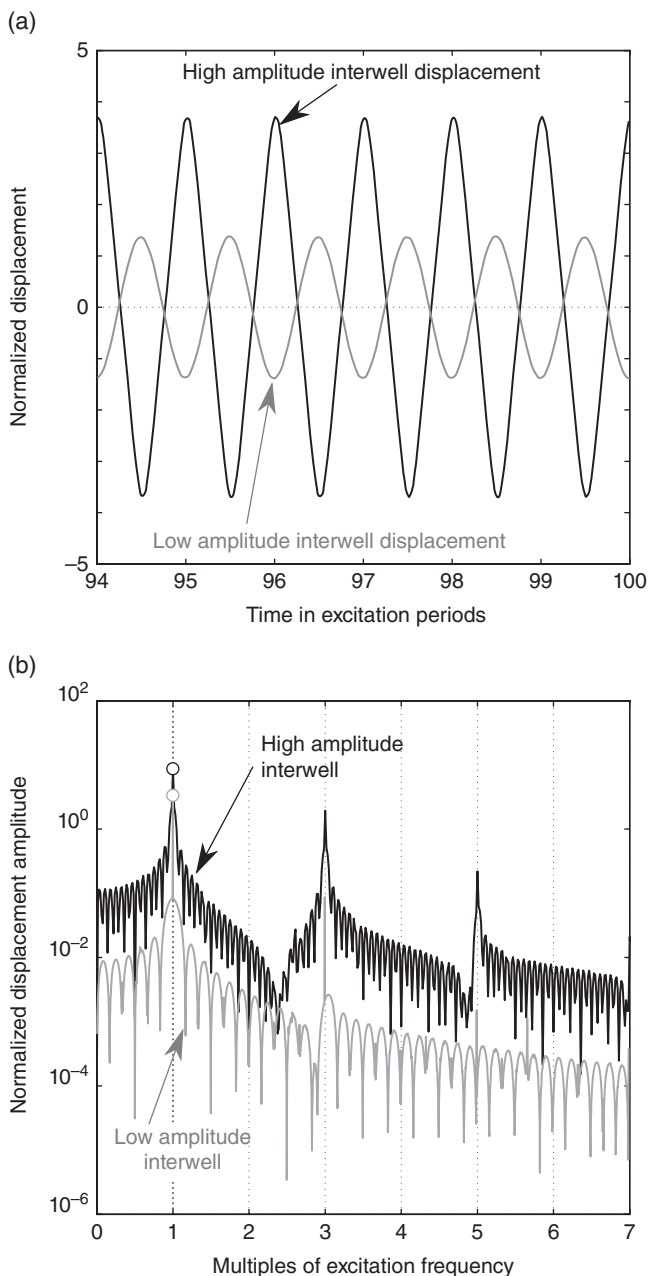
(a)



(b)



**Figure 1.5** (a) For an excitation frequency at which both the low and high interwell dynamics coexist, the time series of the displacement responses is presented. (b) The displacement magnitude spectral responses of the low and high amplitude interwell dynamics are shown as computed from the time series data plotted in (a). The energy diffusion to other harmonics of the excitation frequency is apparent and distinct between the response forms. In (a, b), the parameters are $(p, \omega, \gamma, \beta) = (8, 2.5, 0.09, 1)$, with initial conditions $(-1.9297, -0.0944)$ for the low amplitude interwell responses and $(x_0, \dot{x}_0) = (-2.9443, -0.1791)$ for the high amplitude interwell vibrations.

of the two dynamic forms, it is clear that the responses are approximately 180 degrees out-of-phase. Although not shown in Figure 1.5a, the high amplitude snap-through dynamics occur with phase lags no greater than 90 degrees with respect to the excitation, while the low amplitude interwell oscillations lag the excitation typically by around 180 degrees. The unique phase relationships enable a practical means to distinguish the two forms of interwell dynamics during experimentation in which case they both oscillate back-and-forth across the unstable equilibrium but clearly have different phase relationships with respect to the excitation. Similar to the intrawell dynamic spectral features, Figure 1.5b shows that the two interwell dynamics of bistable systems are different in terms of response amplitude at the excitation frequency of $\omega$ (shown as the circle points) as well as in terms of the energy diffusion to other integer multiple harmonics of the excitation.

By evaluating Eq. (1.1) over a broad range of excitation frequencies using an analytical strategy, Figure 1.6a plots the normalized displacement amplitudes of a bistable system (shown as solid curves) as compared to the linear system governed by the corresponding normalized governing equation of motion $\ddot{x} + \gamma \dot{x} + x = p \cos \omega \tau$ (dash-dot curve). Additionally, Figure 1.6a shows thin gray curves which represent *unstable* dynamics of the bistable system. In other words, these are responses which are mathematical solutions to the governing equations but which are not physically realizable dynamics.

The amplitudes of the bistable system intrawell dynamics show resonance-like frequency dependence similar to the linear system, but the prior are "bent" towards lower frequencies. This is an indicator of a "softening" type of nonlinearity, further details of which are provided in later chapters of this book. It is also observed in Figure 1.6a that the high amplitude interwell dynamics exhibit large displacement magnitudes over a broad range of frequencies. In fact, the large amplitude snap-through dynamics are predicted to occur even for a progressively vanishing excitation frequency, in other words as $\omega \rightarrow 0$. This prediction may be intuitively appreciated through a basic consideration of the mechanics involved. Note that as the frequency approaches zero, the motions of the linear system mass are confined to how greatly the linear spring may be statically deformed for the applied load. In contrast, as the excitation frequency approaches quasi-static conditions, the displacements of a bistable system mass will still undergo a large stroke from one stable equilibrium to the other so long as the system is "pushed" with a large enough load level to induce a snap-through dynamic. As such, it may be stated that snap-through is a *non-resonant* dynamic because there is no reliance on resonance-like features to excite the energetic motions. The exceptional sensitivity to broadband and low frequency inputs is a repeatedly exploited feature of bistable systems in the technical areas described in this book.

A major difference between the responses of the bistable structure and the counterpart linear oscillator are the *bifurcations* in the bistable system responses, observed in consequence to variation in the excitation frequency, $\omega$. A bifurcation is a large qualitative change in a system state (static and/or dynamic) due to an infinitesimally small change in an individual parameter (whether internal or external to the system) [15,16]. Three bifurcations in the dynamics of the bistable

system are apparent in Figure 1.6a. The first is seen to occur where the low amplitude intrawell oscillations destabilize if the excitation frequency exceeds $\omega \approx 1.1$. While the linear system exhibits smooth and continuous variation of displacement amplitudes as the excitation frequency is varied, the bistable system dynamics will undergo a sudden jump from low (point B) to high amplitude
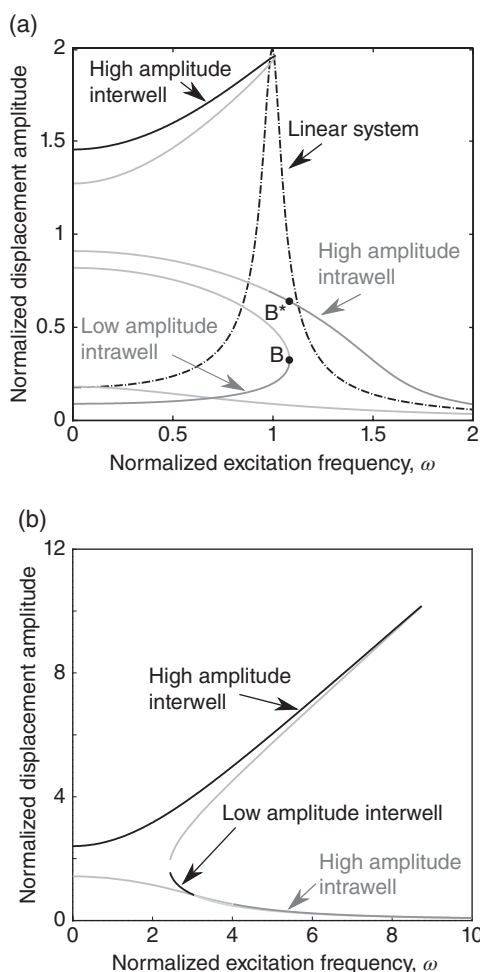
(a)



(b)



**Figure 1.6** Depending on the excitation level, the single-periodic, steady-state response of a bistable system may exhibit non-unique dynamic forms. (a) A high amplitude interwell and both low and high amplitude intrawell responses may occur depending on the excitation frequency. Here, the parameters are $(p, \gamma, \beta) = (0.18, 0.09, 0.7)$. The corresponding linear system stationary response computed using the counterpart equation $\ddot{x} + \gamma\dot{x} + x = p\cos\omega\tau$. (b) A greater excitation level than that used in (a) may induce low or high interwell responses or an intrawell response. Here, the parameters are $(p, \gamma, \beta) = (8, 0.09, 1)$. (c) Responses of softening and hardening Duffing oscillators contrasted against the corresponding linear system. Here, the parameters are $(p, \gamma, \beta) = (0.18, 0.09, 0.7)$. The thin gray curves indicate unstable response forms.
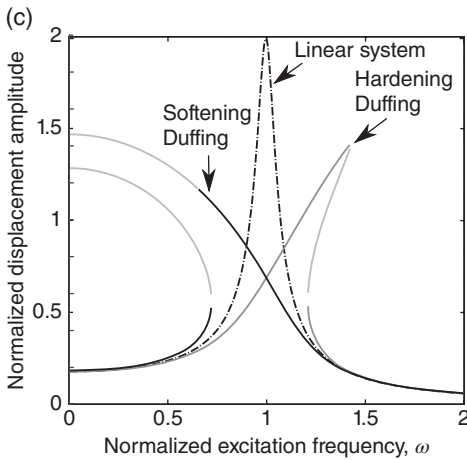
(c)



**Figure 1.6** (Continued)

(point B\*) intrawell oscillations when the frequency exceeds $\omega \approx 1.1$. Another bifurcation is evident in the high amplitude intrawell response if the excitation frequency decreases below $\omega \approx 0.95$; if the frequency is swept below this critical point, the system is predicted to undergo either low amplitude intrawell oscillations or snap-through. The final bifurcation featured in the plot occurs in this bandwidth when the bistable structure is initialized in the high amplitude interwell dynamic state and the excitation frequency exceeds $\omega \approx 1$. This latter bifurcation from an exceptionally large amplitude response (snap-through) to an intrawell dynamic is a distinct characteristic of bistable systems, and the significant response amplitude difference involved can be favorably exploited in several scientific and engineering contexts. For the previous two bifurcations where three, coexistent steady-state responses are reduced to two, the initial conditions at the time of bifurcation activation determine into which dynamic response the bistable system settles.

Figure 1.6b shows results predicted using different system and excitation parameters, and indicates that the low and high *interwell* dynamics may coexist near an excitation frequency of $\omega \approx 2.5$. It is found that the low amplitude interwell oscillations occur across a narrow bandwidth of excitation frequencies. The trend for the high amplitude interwell dynamics is a nearly linear increase in displacement magnitude as the excitation frequency progressively increases. This trend continues up to a critical frequency at which the single-periodic snap-through behaviors become destabilized: a similar bifurcation feature as that observed in Figure 1.6a. Finally, the results plotted in Figure 1.6b show that a high amplitude intrawell dynamic is possible for excitation frequencies greater than $\omega \approx 4$. The phase relationship of these intrawell oscillations with respect to the excitation is the characteristic factor to identify the dynamic regime.

The analytically predicted results in Figure 1.6 provide a clear example of the coexistence of numerous, steady-state dynamic forms of bistable structures as well as the possibility for sudden transitions in the dynamic regime due to small

changes in system or excitation parameters. The multiplicity of the response forms, characterized by their unique displacement amplitudes and excitation phase lags, makes bistable structural dynamics particularly distinct from those of other linear and nonlinear systems. Indeed, snap-through is truly a distinguishing feature of bistable systems.

It is worthwhile to compare the steady-state, single-periodic dynamics of bistable structures to those of the traditional hardening and softening Duffing oscillators, which are regularly implemented as archetypal models for engineering systems in the real-world [17,18]. These oscillators are governed by the equations $\ddot{x} + \gamma\dot{x} + x \pm \beta x^3 = p\cos\omega\tau$ where the positive (negative) nonlinear restoring force term denotes hardening (softening) behavior. It is evident that this governing equation is similar to Eq. (1.1) for the bistable system, repeated here for convenience: $\ddot{x} + \gamma\dot{x} - x + \beta x^3 = p\cos\omega\tau$. On the other hand, the resulting static and dynamic behaviors are considerably distinct. Note that the only static solution to the equations $\ddot{x} + \gamma\dot{x} + x \pm \beta x^3 = p\cos\omega\tau$ is $x = 0$, indicating that the Duffing systems have just one static equilibrium and are thus termed *monostable*. Using the methods presented in Chapter 2, the steady-state dynamics of the forced Duffing equations may be approximately solved and representative results are shown in Figure 1.6c using parameters of $(p, \gamma, \beta)$ identical to those used in Figure 1.6a. Here again, the corresponding linear system dynamics are also shown, and light gray curves denote the unstable behaviors of the Duffing systems. Figure 1.6c illustrates that the hardening Duffing oscillator exhibits a "bending" or "leaning" of the resonance curve to higher frequencies with respect to linear system trends. In contrast, the softening Duffing oscillator shows response amplitude curves that lean to lower frequencies. Figure 1.6c indicates that the Duffing systems may exhibit *dynamic bistability*, in that more than one steady-state oscillation regime may occur for a given excitation frequency (similar results are obtained by varying the other parameters $\beta$, $\gamma$, and $p$). In comparing the different responses of bistable and these *monostable* Duffing oscillators between Figures 1.6a and 1.6c, respectively, it is evident that the intrawell oscillation regime of the bistable system is comparable to the softening Duffing response, while the Duffing oscillators exhibit no such dynamic behavior as snap-through since the Duffing systems do not possess *static bistability*. Truly, it is static bistability that enables snap-through and draws a dramatic distinction in the resulting, potential dynamic behaviors of bistable systems which the following sections continue to detail.

### 1.2.2   Sensitivity to Initial Conditions

It was shown in Figures 1.4 and 1.5 that system and excitation parameters as well as the initial conditions influence the resulting dynamic state of a bistable system. In fact, this is a characteristic of all nonlinear systems which may exhibit multiple coexistent steady-state dynamics. On the other hand, due to the two stable equilibria, there are important implications of the initial condition sensitivity demonstrated by bistable structures. A clear example of this feature is shown in Figure 1.7 where a difference in initial normalized displacement of $10^{-6}$ leads to completely different results as time elapses. It is seen that, based on the
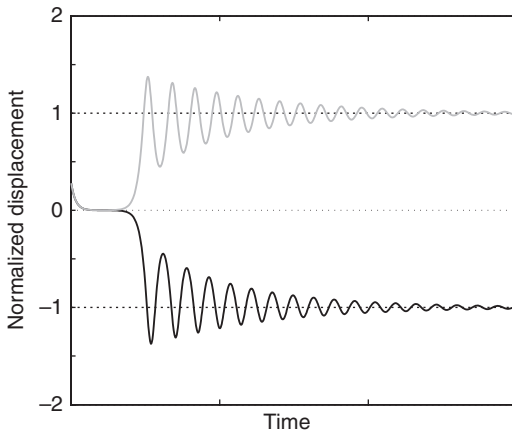
**Figure 1.7** The transient responses of bistable systems may exhibit high sensitivity to initial conditions. In this example, the initial conditions are $(x_0, \dot{x}_0)=(0.292721, -0.3)$ for the response settling to the normalized displacement stable equilibria position of −1 (black curve), while the small change of initial conditions to $(x_0, \dot{x}_0) = (0.292722, -0.3)$ causes the transient dynamics to tend to the stable equilibrium of normalized displacement +1 (gray curve). Here, the parameters are $(\gamma, \beta) = (0.09, 1)$. The thick dotted lines indicate the statically-stable equilibria.

initial displacement, the unforced, transient dynamics of the oscillating mass decay and ultimately come to rest at one of the two stable equilibria. Thus, unlike the initial condition sensitivity of other nonlinear systems which becomes evident due to *steady-state* excitations, the *unforced* dynamics of bistable structures may be strongly sensitive to changes in initial conditions. The unique final value of normalized mass displacement is also relevant in the event that the bistable system is harmonically-excited. As was described in Section 1.2.1, the low or high amplitude intrawell dynamics may be realized as oscillations around either of the stable equilibria, which means that the average value of the steady-state dynamic is unique. All together, the initial condition sensitivities of bistable systems are manifest in distinct ways as compared to other nonlinear systems, because the offset or bias of the inertial mass due to the stable equilibria is a trademark characteristic of bistable structures.

### 1.2.3 Aperiodic or Chaotic Oscillations

When subjected to single-frequency excitations, certain classes of nonlinear systems may oscillate aperiodically. These motions are not to be confused with noise-induced behaviors and may indeed appear to be completely random. Yet, they can be deterministically predicted using the system governing equation and knowledge of the initial conditions. This phenomenon can be classified and quantified as *chaos*, and it occurs for a variety of physical, fluid, electrical, chemical, optical, and acoustic systems [19]. When it is possible, chaos is not always the dynamic form which is exhibited due to single-frequency excitation. Comparable to the potential for coexistent steady-state dynamic regimes exemplified in Figure 1.6, a specific set of system and excitation parameters can lead to aperiodic

responses in a bistable system. However, the analytical tools to predict the steady-state dynamics in Figure 1.6 are incapable of identifying chaotic dynamics because such analytical techniques assume the dynamics of the bistable system are periodic. Consequently, a common strategy is to numerically integrate the governing equations when chaos is anticipated to approximate the parameter dependence of realizing chaotic responses for bistable structures. The manifestation and importance of chaos for the engineering implementation of bistable systems is described below.

The chaotic dynamics exhibited by bistable systems are realized as aperiodic interwell behaviors. As a first look into the features of chaos for a bistable system, Eq. (1.1) is numerically integrated using two slightly different sets of initial conditions and the computed displacement trajectories are plotted in Figure 1.8. There are several aspects to observe. First, the dynamics are clearly aperiodic although the input excitation is a single sinusoidal motion. Even after 500 cycles of excitation, Figure 1.8b shows that the displacement responses maintain an apparently random nature. The behaviors are not to be confused with a prolonged decay of transient dynamics related to initial conditions because the bistable system has appreciable damping. Continued numerical integration of the governing equation shows that the aperiodicity is maintained. In addition, the initial condition sensitivity of the chaotic responses as time progresses is exemplified in Figure 1.8a where two aperiodic displacement trajectories are seen to diverge after about 10 cycles of excitation. Following 500 periods of excitation, Figure 1.8b shows that there is little resemblance between the results. Although not shown in the example in Figure 1.8, a feature may be exhibited where chaos is realized in brief bursts. This *transient chaos* phenomenon occurs when intrawell dynamics of the bistable system appear to be the established steady-state response, but then a sudden and temporary bout of aperiodic interwell responses may be activated. The engineering implications of transient chaos are important because large amplitude chaotic dynamics may suddenly overtake an otherwise predictable intrawell dynamic of the bistable structure. In addition, once the transient chaos passes and the intrawell behaviors re-emerge, the system might in fact oscillate around the other stable equilibrium. Thus, an instance of transient chaos may lead to a change in the static state of the bistable system once the phenomenon has passed (should the excitations be removed). Such potential for state change is unique to the bistable structural systems which exhibit chaos. Although it is important to understand the potential for chaos, to date there have been few practical implementations of chaos for bistable systems in the technical areas of interest in this book. Engineers in vibration control, energy harvesting, and sensing typically avoid design and operational regimes that may induce chaotic dynamics. Interested readers are encouraged to refer to other works for further details regarding the chaotic dynamics of bistable structures [19–23].

### 1.2.4 Excitation Level Dependence

The forced, steady-state dynamics of nonlinear oscillators often exhibit an intricate dependence on the level of excitation. Whereas the response magnitudes of linear systems change with direct proportionality to the excitation level, the
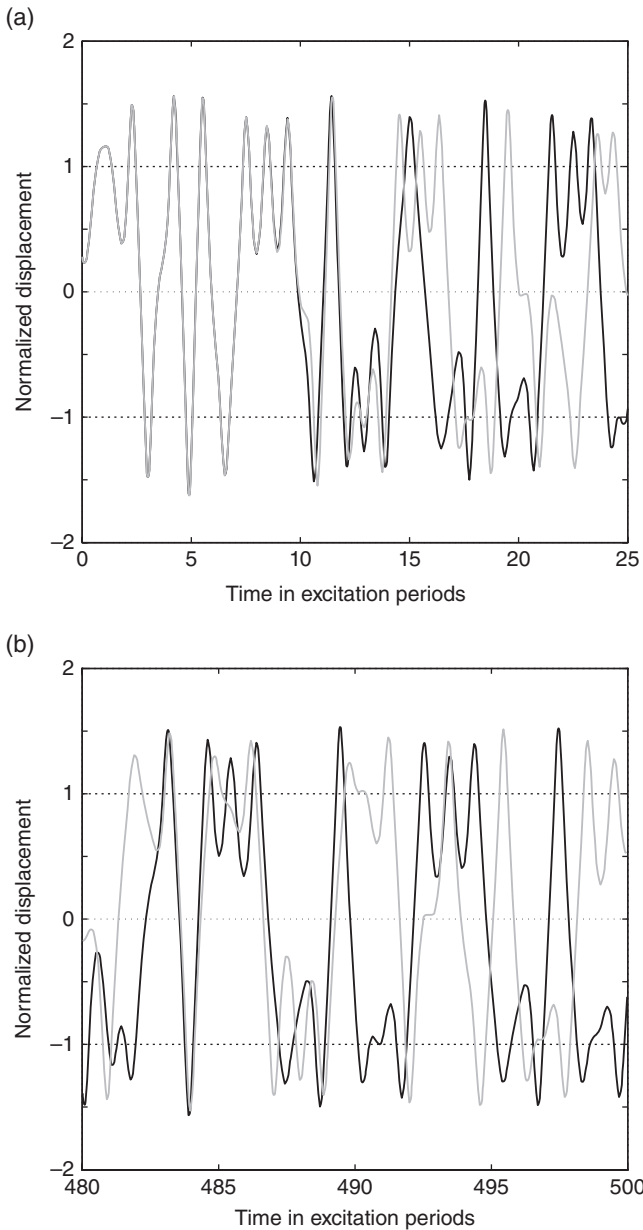
(a)



(b)



**Figure 1.8** (a) An harmonically-excited bistable system may lead to aperiodic dynamics. This characteristic is also strongly sensitive to initial conditions. Thus, after only a small number of excitation periods, two nearly identical initial conditions show great divergence in the transient, aperiodic snap-through dynamics of the bistable systems. (b) After 500 excitation periods, the aperiodic responses bear little resemblance. Here, the parameters are $(p, \omega, \gamma, \beta)=(0.37, 1.29, 0.1, 1)$, with initial conditions $(x_0, \dot{x}_0) = (0.292707, -0.3)$ leading to the responses plotted in the black curves and with initial conditions $(x_0, \dot{x}_0) = (0.292706, -0.3)$ leading to the responses plotted in the gray curves. The thick dotted lines indicate the statically-stable equilibria. The normalized sampling frequency in the 4th-order Runge–Kutta numerical integration is 32.

dynamic amplitudes of nonlinear systems as well as the existence of a given dynamic form will, in general, vary non-proportionally due to excitation level change. Because of the multitude of single-periodic behaviors that bistable systems may exhibit, the excitation level dependence is critical to examine for a bistable structure applied in an engineering practice. In other words, it is essential to determine the suitable design and excitation conditions that help to ensure the desired dynamic form is activated and the target performance objectives are achieved.

Figure 1.9 provides an example of the excitation level dependence of a bistable system. The analytically predicted results are computed for three excitation frequencies. Figure 1.9a shows the results for frequency $\omega = 0.8$ while Figure 1.9b,c show results for $\omega = 1$ and $\omega = 1.2$, respectively. The data for the bistable system are shown as solid curves whereas the counterpart linear system responses are identified by the dash-dot curves. Comparable to the excitation *frequency* dependence illustrated in Figure 1.6, the excitation *level* is an important parameter to determine the occurrence of the unique dynamic forms of the bistable structure; in Figure 1.9 these dynamic types are the low and high amplitude intrawell oscillations and the high amplitude interwell, snap-through vibrations. For the case of excitation frequency at the resonance-like condition, $\omega = 1$, shown in Figure 1.9b, the peak amplitudes which may be achieved for the high amplitude intra- and interwell dynamics of the bistable system are nearly identical to the response of the linear system excited at resonance. On the other hand, when excited off-resonance such as $\omega = 0.8$ or 1.2, Figure 1.9a,c, respectively, the dynamics of the bistable structure, and in particular the interwell snap-through vibrations, may achieve substantially greater amplitudes for the same excitation level. For the scientist or engineer who wishes to exploit the large, steady-state amplitudes of displacement enabled by a bistable system's snap-through characteristics, it is clear that an intelligent assessment of the excitation conditions under which the platform will operate – both the level and frequency of the forcing – is required to ensure the activation of the energetic behaviors.

Another informative assessment metric of the excitation level dependence for nonlinear systems is the frequency response function (frf), which is often computed as the ratio of a response magnitude (e.g., displacement, velocity, or acceleration) to the excitation level. As an example, Figure 1.10 plots the displacement frf magnitude of a bistable system (solid and dashed curves) as compared to that determined for a linear system (dash-dot curve). It is clear that the linear system response amplitudes are independent of the excitation level, as anticipated from a fundamental understanding of system dynamics. In contrast, due to the variation in excitation level, the bistable system displacements change in terms of frf amplitude as well as the frequency bandwidths across which each dynamic regime occurs. The arrows on the plot indicate the trend of change as the excitation level is increased. It is seen that increasing excitation level reduces the maximum frequency of existence for the low amplitude intrawell oscillations and increases the minimum frequency of existence for the high amplitude intrawell oscillations: a gap in the frequency bandwidth thus occurs across which only the snap-through dynamics are anticipated. At the same time, as the excitation level increases the snap-through dynamics are predicted to be sustained to higher frequencies. Additionally, the frf magnitude of the snap-through displacement

response reduces. Thus, from Figure 1.10 it is clear that the maximum amplitude of the frf of bistable system snap-through dynamics is most nearly equal to that of the linear system only for low excitation levels when considering the resonance-like excitation frequency $\omega = 1$. On the other hand, the realization of the snap-through dynamic is more greatly ensured as the excitation increases because the frequency bandwidth of coexistence with intrawell dynamics is found to reduce. The excitation level dependence characteristics illustrated in Figure 1.9 and Figure 1.10 are important to understand in order to appropriately harness the distinct bistable structural dynamics for engineering applications.
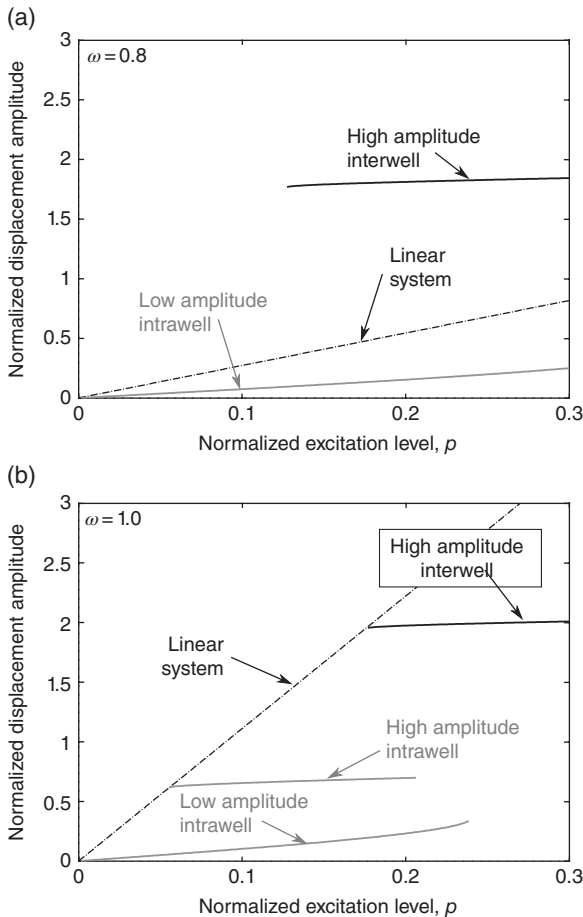


**Figure 1.9** Depending on the excitation frequency, the single-periodic, steady-state response of a bistable system may exhibit non-unique dynamic forms. In the following examples, changes in normalized excitation frequency $\omega$ lead to variation in the amplitude and existence of the low and high amplitude intrawell dynamics and the high amplitude interwell vibrations of a bistable system, as functions of changing normalized excitation level $p$. In contrast, only the amplitude of the counterpart linear system responses is seen to vary. Results computed for (a) a normalized excitation frequency $\omega = 0.8$, (b) $\omega = 1.0$, and (c) $\omega = 1.2$. Here, the parameters are $(\gamma, \ \beta) = (0.09, 0.7)$. The corresponding linear system stationary response computed using the counterpart equation $\ddot{x} + \gamma \dot{x} + x = p \cos \omega \tau$.

(c)
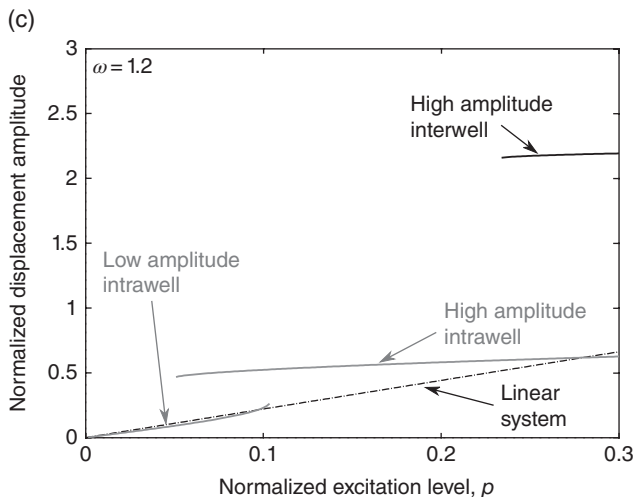


**Figure 1.9** (Continued)
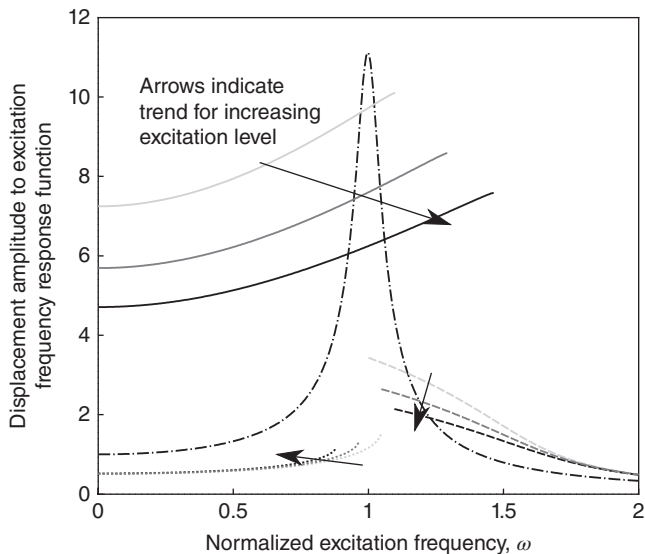


**Figure 1.10** Examples of the frequency response function (frf) dependence of a bistable system as compared to a linear system. The frf is the displacement amplitude with respect to the excitation level. The linear system frf (dash-dot curve) is independent of excitation level. For bistable systems, the interwell response frfs (solid curves) reduce in amplitude but extend to higher frequencies as the excitation level increases. The high amplitude intrawell frfs (dashed curves) reduce in amplitude and frequency range as the excitation level increases, while the low amplitude intrawell dynamics (dotted curves) primarily reduce in frequency bandwidth without notable change in frf level. The light to dark curves for the bistable system are determined using $p$ from 0.17, 0.22, to 0.27. Here, the parameters are $(\gamma, \beta) = (0.09, 1)$. The linear system frf is computed using damping factor $\gamma = 0.09$.

### 1.2.5 Stochastic Resonance

Although Section 1.2.4 indicated that greater excitation levels may help to consistently activate the snap-through dynamics of bistable systems by reducing the likelihood that intrawell dynamics could coexist, there is an additional avenue to realize the energetic interwell behaviors. The phenomenon is called *stochastic resonance* and it is a thoroughly investigated feature of bistable systems, particularly in physics-based research [24,25]. Stochastic resonance refers to the effect of exciting a bistable system with a combination of low-level, single-frequency harmonic input and low-level noise so as to activate snap-through dynamics. Individually, the two excitation inputs are insufficient to induce the interwell behaviors but their combination has dramatic influence.

Figure 1.11 shows an example of this dynamical feature. It is seen that the individual periodic or white Gaussian noise excitations upon the bistable system lead only to low amplitude oscillations around one of the two stable equilibria, whether they are periodic or stochastic in nature. However, in combination, the excitations activate snap-through dynamics. By considering the normalized time axis and the times at which the snap-through transitions occur, it is also apparent that the resulting large amplitude motions occur primarily at the same frequency as the periodic input. As a result, this phenomenon provides a novel avenue to magnify a low-level input by the "injection" of either noise or periodic excitations to activate the high amplitude interwell dynamics in the bistable system with a minimum of extra cost in terms of the input energy. Stochastic resonance is not unique to nonlinear systems exhibiting bistability [24], but the degree of response amplification that bistable structures may realize due to
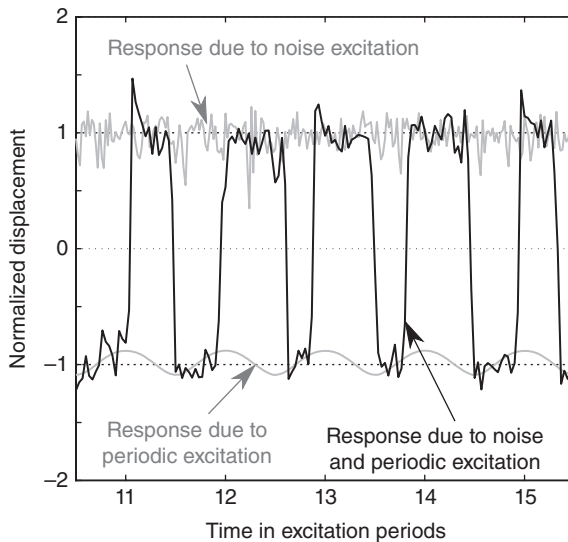


**Figure 1.11** The stochastic resonance phenomenon occurs when combined periodic and stochastic excitations, which are individually insufficient to activate snap-through dynamics of a bistable system, lead to large amplitude interwell dynamics which closely follow the excitation period of the periodic excitations. Here, the parameters are $(p, \omega, \gamma, \beta) = (0.2, 0.05, 0.5, 1)$ for the cases involving the periodic excitations. The normalized, additive white noise variance is 0.04. All cases use initial conditions $(x_0, \dot{x}_0) = (0, 0)$.

stochastic resonance is notably greater because of the switching back and forth between the two stable equilibria. This distinction is one reason for the increased attention on stochastic resonance in the context of bistable structures and systems throughout the scientific and engineering fields.

### 1.2.6 Harmonic Energy Diffusion

The results presented in Figure 1.4b and Figure 1.5b indicate that the four, steady-state types of bistable structural dynamics are distinct in terms of their respective amplitudes. Looking closer at the spectral plots, it is also apparent that the input energy at frequency $\omega$ becomes manifest via dynamics of the bistable structure at other frequencies. In other words, the energy is *diffused* from the single-frequency input to other harmonics. Specifically, for the intrawell dynamics Figure 1.4b shows that the input energy becomes concentrated in the system dynamics at integer multiples of the excitation frequency. In this case, the input excitations at a frequency $\omega$ are exhibited by bistable system dynamics at frequencies $n\omega$ where $n = 1, 2, 3,\ldots$ It is also evident in Figure 1.4b that the high amplitude intrawell dynamics exhibit a greater degree of such energy diffusion than the low amplitude responses.

Similar results are seen in Figure 1.5b where the coexistent low and high amplitude interwell dynamics diffuse the input energies at frequency $\omega$ to responses at frequencies $m\omega$ where $m = 1, 3, 5,\ldots$ In the cases presented in Figures 1.4b and 1.5b, the harmonic energy diffusion is not dramatic because the corresponding time series plots, Figures 1.4a and 1.5a, show that the bulk of the dynamic behaviors is indeed at the same frequency of excitation, albeit with phase shifts. (One may verify this conclusion by comparing the primary periods of the displacement responses to the horizontal axes which are shown as time in normalized excitation periods). Nevertheless, the spectral results reveal that the bistable system redistributes a non-trivial amount of the input energy into dynamics at other frequencies.

Yet, in some cases, the harmonic energy diffusion may become extreme. Figure 1.12 provides clear examples of this possibility such that the single-frequency input at $\omega$ is mostly concentrated at other frequencies. Figure 1.12a shows that for some system and excitation parameters, the inputs at frequency $\omega$ become primarily concentrated at frequency $\omega/3$ (black curve) or $2\omega$ (gray curve). The time series results plainly reveal that the dynamics which achieve such significant harmonic energy diffusion are interwell behaviors, and specifically large amplitude snap-through effects. In Figure 1.12b, the spectral results computed from the corresponding displacement time series verify the dramatic redistribution of input energy via the particular manifestation of bistable system dynamics. It is seen that in the one case, the energy is predominantly redistributed to frequencies $m\omega/3$ where $m = 1, 3, 5,\ldots$ (black curve), while in the other case the spectral peaks occur at $2m\omega$ (gray curve). No less important than when the energy remains primarily concentrated at the excitation frequency, the extreme harmonic energy diffusion due to bistable system snap-through dynamics has critical engineering implications for their appropriate utilization.

In general, the redistribution of the dynamics from a single-periodic response to a variety of frequencies is not unique to bistable systems and can be exhibited

(a)



(b)
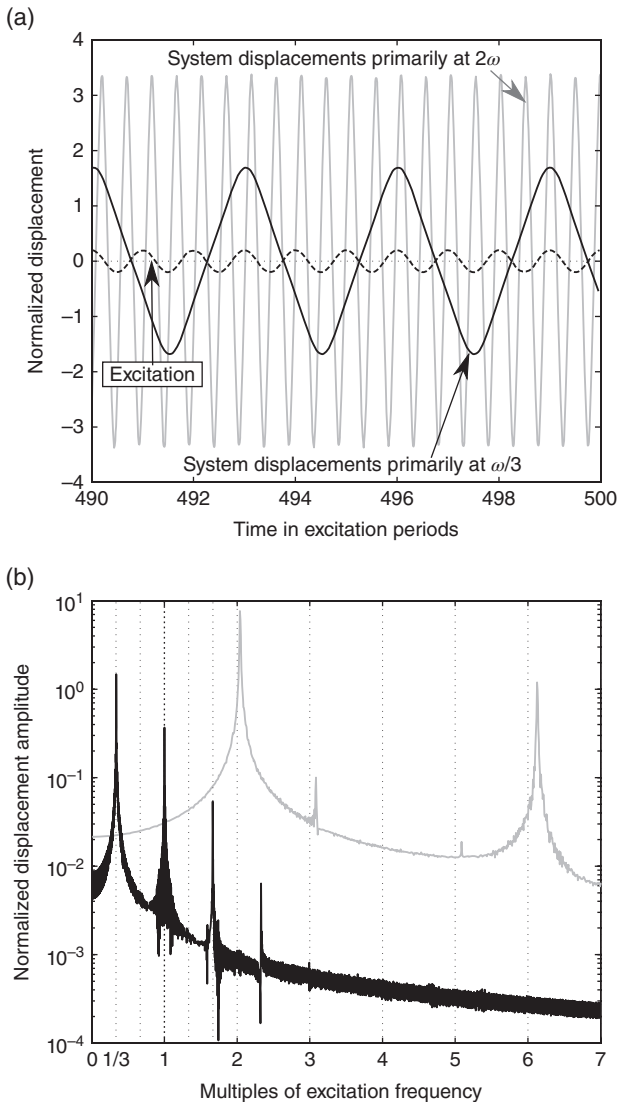


**Figure 1.12** (a) Although bistable systems may be excited at a frequency $\omega$, the steady-state dynamics may occur primarily at integer multiples or fractions of the excitation frequency. Two cases are shown for which the system primarily vibrates at a frequency of $2\omega$ (gray curve) or $\omega/3$ (black curve. (b) The displacement magnitude spectral responses of the bistable system dynamics, as computed from the time series data plotted in (a), show clearly the unique spectral concentrations of the input excitation energies. In (a,b), for the dynamics tending to the frequency of $2\omega$, the parameters are $(p, \omega, \gamma, \beta) = (0.2, 1.3, 0.0001, 1)$, with initial conditions $(x_0, \dot{x}_0) = (-3.2987, 1.5132)$; while for the dynamics tending to the frequency $\omega/3$, the parameters are $(p, \omega, \gamma, \beta) = (0.2, 3, 0.01, 1)$ with initial conditions $(x_0, \dot{x}_0) = (-0.7507, 1.4841)$.

by other nonlinear systems. On the other hand, the multitude of the possible, coexistent steady-state dynamic forms of bistable structures lends itself to an intricate manifestation of harmonic energy diffusion that is not evident in other

nonlinear systems. This provides bistable systems with a much greater variety of multiharmonic dynamic characteristics that may be intelligently harnessed.

## 1.3 The Exploitation of Bistable Structural Dynamics

The review above indicates that the dynamics of bistable systems include a rich assortment of behaviors. All together, the numerous distinct features suggest that an attractive versatility of response may be exploited by intelligently utilizing or switching among the different types of dynamics that are realized by a single degree of freedom (DOF), bistable architecture. As compared to the considerably more uniform response characteristics of linear systems and the fewer opportunities to exploit with other nonlinear platforms, the dynamics of bistable structures and the various means by which to realize bistability motivate the scientific and engineering utilization of bistable system architectures to advance a variety of technical fields.

The rationale for exploiting bistable structural dynamics depends upon the application. In some cases, the reasons that encourage use of certain dynamic forms are the same that could discourage their use for other purposes. Therefore, the perspective of the researcher and the performance metrics of interest are the guiding factors for appropriately harnessing bistable system dynamics. Across the fields of vibration control, vibration energy harvesting, and sensing, there are certain shared or underlying aims that the dynamics of bistable systems have been found to meet effectively in ways and to degrees beyond what is possible when utilizing alternative system platforms.

The shared aims may broadly be described as achieving exceptionally *energetic responses* and enabling *adaptability*. For bistable structures, the basis for realizing notably energetic responses is the opportunity to activate snap-through dynamics, which do not have a counterpart in single DOF linear or other monostable nonlinear systems. The adaptability of bistable system dynamics is due to the potential for multiple, coexistent steady-state responses – whether they are single-periodic, multiharmonic, or aperiodic – such that an intelligent exploitation of system design and excitations can enable one to selectively trigger the dynamics that are preferred for a certain operating condition or application.

In the technical areas of interest in this book, the energetic responses and adaptability of bistable structural dynamics draw the several engineering applications around the general objectives of enhanced performance versatility and functionality. In the following sections, the individual aims of vibration control, energy harvesting, and sensing applications are briefly detailed. Within each context, a first look is taken at how the objectives of the areas have recently been achieved and advanced through the exploitation of bistable system dynamics, particularly as they relate to harnessing the energetic and adaptable responses.

### 1.3.1 Vibration Control

Dissipating, isolating, or absorbing the vibrations of structures is an historic goal: elastic carriage suspensions were employed during, if not also before, the Iron Age [26], while the first example of a vibration absorber for reactive attenuation

purposes is often dated to Hermann Frahm's patent in 1910 for an anti-roll tank for ships [27]. Apart from the assurance of comfort via limiting the jarring of carriage vibrations or alleviating the possibility of sea-sickness, the control of vibrations is more recently a matter of structural necessity.

The use of engineering systems in ways or in environments that cause significant vibration levels, for example space vehicle launches or even the ordinary operation of rotorcraft, requires that vibration control systems operate effectively and with high performance to ensure the success or integrity of the structure in its mission. The numerous costs associated with energy to fuel a wide variety of vehicular systems, including aerospace, marine, and automotive vehicles, have stimulated the use of lightweight structures and materials to minimize mass to allowable safety standards. This means that the inherent energy dissipation characteristics of the system are of great importance. Without sufficient, and oftentimes high, damping capacity in the lightweight systems, the day-to-day operation of many modern engineering structures and materials carries the risk of incurring a catastrophic failure due to working too closely to the limits of system integrity. On the other hand, although high damping is critical for some applications, low damping may be just as vital. For example, the need to obtain accurate wave- or vibration-based signal readouts from a structure to monitor its operating state, also termed structural health monitoring, benefits from a lightly damped structure at the time of data acquisition for the sensors to acquire clear measurements. As a result, modern implementation of engineering systems has led to a set of operational requirements for vibration control performance, some conflicting with each other: for instance, a lightweight structure or material solution that provides high damping during rotorcraft operation but low damping during a rotor blade condition monitoring examination.

From age to age, the achievement of these overall vibration control aims has been limited by the traditional employment of passive materials or devices having tightly prescribed capabilities, often as a result of operating the system within a linear dynamic regime. The introduction of nonlinear components for energy dissipation, such as fluid [28] or friction dampers [29], led to improved performance potential, particularly for high vibration levels. Nevertheless, the more extensive exploration and exploitation of nonlinear vibration control concepts, including the harnessing of bistable elements, is a comparatively recent initiative [30,31].

Indeed, there are a variety of advantages to be gained by employing a bistable device in its own right within the architecture of a vibration damping, isolation, or control system. The energetic snap-through dynamics lead to high velocity motions for the inertial mass, due to the large displacement strokes from one stable equilibrium to the other and associated low dynamic stiffness. In addition, snap-through is activated across a broad bandwidth of frequencies when compared to a linear system and its resonant dynamics, as exemplified by Figure 1.6. Collectively, these characteristics of large kinetic energy, low dynamic stiffness, and potential for adaptively triggering large amplitude, periodic motions provide opportunities to advance aims in dissipating, isolating, and absorbing vibrations in myriad contexts.

One idea recently explored to achieve damping characteristics uncommon in traditional bulk materials is the implementation of bistable elements into structural or material systems to take advantage of the snap-through dynamics.

In such implementations, the bistability of the system is deliberately retained. In these initiatives, by capitalizing on the activation of snap-through dynamics of an inertial mass, a large dissipation of energy is realized: extreme damping. This idea has been theoretically and experimentally explored using numerous incorporations of bistable elements into the systems, such as negative stiffness inclusions within a host material matrix [32] and as an integrated device composed of bistable structures in parallel with dampers [33,34], to sample only a couple of the various system realizations. The broadband spectral characteristics of snap-through motions provide a particular motivation for their exploitation to enable a high damping capacity. As described in Section 1.2.1, snap-through is a non-resonant dynamic which means there is no reliance on resonance-like phenomena to achieve the large amplitude interwell motions: only a sufficient excitation level is required to induce the energetic state change from one stable equilibrium to the other. Thus, incorporating bistable elements into a structural or material system provides the means for cultivating high damping properties across a wide range of excitation frequencies.

As described above, modern engineering systems that require high damping may also benefit from an intrinsic ability to tailor energy dissipation or vibration suppression characteristics. Although active control systems may be used to effect real-time variations in the dynamic characteristics of engineered structures, there are significant advantages to developing and employing passive-adaptive systems that are inherently multifunctional via mechanical properties tuning. In this way, the system weight remains low and complexity is alleviated because the properties of the system may be adapted passively without need for the weight, maintenance, and energy expense of active control hardware. By exploiting the excitation level and frequency dependence of the snap-through dynamics of bistable structures, one may realize adaptable harmonic energy dissipation features [34]. A simple implementation of the concept is described following the basic trends shown in Figure 1.9. Thus, for a structure with bistable damper inclusions a small dissipation of energy is realized when the excitation level is low, but as the level increases the activation of snap-through dynamics can be harnessed for more aggressive levels of damping. Careful investigations of damping and excitation level dependence on the snap-through characteristics of bistable systems [35,36] have provided informative guides to achieve adaptable damping features.

Bistable systems with buckled structural members are also leveraged for vibration isolation purposes. The dynamic stiffness near the point of structural buckling is very low to significantly reduce transmitted force and displacement, while the static stiffness of buckled members can be quite large in order to support high load [37,38]. Indeed, the use of buckled components in their own right is straightforward as well as effective when subjected to the range of operational conditions for which they were developed. On the other hand, many applications of vibration isolation involve significant time-variation in the characteristics of the excitation source, whether in terms of primary frequencies or amplitudes. Consequently, researchers are considering strategies by which to enhance the robustness of performance for vibration isolation systems containing bistable components, such as by using combinations of linear and bistable

elastic components [39,40]. In this way, the energetic snap-through dynamics are leveraged in the best ways possible. As revealed in Section 1.2, the dynamics of bistable structures are rich and, as described elsewhere throughout this book, the coupling of bistable components to other linear elastic members may induce even richer opportunity for dynamic response regimes that may be activated according to different operating conditions. Thus, the exploitation of bistable structures for vibration isolation purposes provides a unique high-risk, high-payoff context that researchers are investigating in detail and with enthusiasm.

Another extension upon the idea of bistable structural integrations for high performance vibration control is the idea to employ snap-through dynamics as a mechanism for vibration absorption. This initiative stems from the established understanding of the operating principles of classical vibration absorbers: the attachments suppress the motions of the excited host system to which they are attached via forces the absorbers generate, which are equal in amplitude and opposite in phase with respect to those produced by the harmonic excitations. As the logic then follows, a bistable vibration absorber employing large amplitude and broadband snap-through dynamics may have particular advantages for reactive vibration control purposes if the dynamics are suitably harnessed in such a way as to supply the needed out-of-phase forces upon the host system. Several researchers have begun to explore this new outlook [41–43] and have so far considered bistable device attachments and primary structures consisting of lumped-parameter constituents, in other words lumped masses, coil springs, and so on. The snap-through dynamics of a bistable system thus open a second avenue of research for vibration control studies, wherein the energetic responses can be intelligently tailored to provide precisely the required reactive force upon a host structure for vibration absorption aims.

The strict and sometimes conflicting standards of high vibration control performance in many modern engineering systems indicate the achievement of the numerous aims using passively-adaptable structural members or integrations is of significant value. The selective activation of energetic snap-through behaviors has been found to be a novel approach to meet the various objectives. The encouraging research results to date serve as strong motivation for the ongoing explorations of harnessing bistable system dynamics in vibration control applications.

### 1.3.2 Vibration Energy Harvesting

The conversion of ambient vibrations, caused by environmental sources or structural motions, into a usable electrical power resource is an emerging technical field. The rapidly growing interest in and attention to vibration energy harvesting opportunities have led to systems and methods that, in the relatively short span of time from the initial explorations, are already at the early stages of commercialization. There are numerous factors that have encouraged the investigations and stimulate the continued efforts.

One motivating factor is to harvest the available vibrational energies to enable low-powered, self-sustainable microelectronics employed in remote or embedded applications where other energy resources are unavailable or inconveniently

accessed via line transmission [44–46]. The sources of such vibration considered are numerous but a sample of such environmental oscillations include: bridge vibrations induced by vehicles, wind loading, pedestrian traffic, and so on; human motions such as walking or jogging; transport vehicle vibrations like aircraft wing oscillations or railway car bearing accelerations. The applications for the electrical energy harnessed from such vibrations include the proliferating implementation of distributed, structural health monitoring nodes and the recent interest in implanted devices like automotive tire pressure sensors or even biomedical devices. The architectures utilizing the harvested energy typically have low power requirements (around mW) due to the efficiency of the electronics, yet would have limited operational life-spans (or fixed intervals of manual service) if powered by conventional batteries that are exhausted over time. By employing electromechanical systems which capture and convert sufficient vibrational energy, one may then use the electrical output to charge a storage element or directly power an electronic system, following a power-conditioning phase.

Another motivating factor in vibration-based energy harvesting is to generate large power (W or greater), and potentially to supplement the conventional, continental electric grid [47,48]. A prime example of vibrations considered by this perspective is the heaving motions of ocean waves. For instance, it is estimated that the overall wave energy resource of western European coastal fronts is itself greater than the world's present-day energy demand ($\sim$2 TW!) [47], assuming it could be adequately concentrated and harvested. Other vibration sources considered in this perspective of energy harvesting are large-scale structural system motions such as the wind- or seismic-induced sway of skyscrapers and automotive suspension motions [49]. Due to the significant attention to and demand for alternative, sustainable energy resources to reduce civilization's reliance on exhaustible supplies, the conversion of vibrational energy for large-scale use is an established area of active research and commercial interest.

In spite of the two different motivating factors, a common aim is apparent: to capture, or additionally amplify, the ambient vibrational energies within an electromechanical energy harvesting system. Once consolidated in this way, the transduced electrical current is conditioned to charge storage elements (for example, rechargeable batteries or capacitors) or directly power a system. The vibrations considered in these studies are commonly periodic or stochastic in waveform. In addition, the electromechanical transduction approaches are typically those which generate an electrical signal due to the relative velocity of the harvester's moving mass, for example, piezoelectric materials on a vibrating cantilever beam or a magnetic mass-spring oscillator moving through a coil. For periodic vibrations, it is logical to use an energy harvesting system that resonates or similarly amplifies the input motions by matching the sensitivity of the harvester dynamic responses to the input vibrations. As a result, early investigations explored linear energy harvesting architectures that resonate at the predominant frequency of the periodic input vibrations. Thus, the sensitivity of the electromechanical systems is appropriately tuned for the input spectrum, a strategy common to both research perspectives in the energy harvesting field. By capturing and ideally amplifying the input motions via a resonant-type energy harvesting platform, a beneficial electromechanical conversion of the vibrations is achieved.

A serious disadvantage of linear resonant harvester systems is the narrow band of frequencies across which the high amplitude dynamics occur. Because the spectral concentration of periodic vibrations changes regularly, for example, due to change in temperature of the host structural system or different human walking gaits, the reliance on a limited frequency bandwidth of high performance makes the practical implementation of linear resonance-based energy harvesting platforms a less than promising approach. Therefore, harnessing the broadband snap-through behaviors of a bistable energy harvester has clear advantages in terms of performance and robustness to changing excitation conditions. As was shown in Figure 1.6a, the large amplitude interwell dynamics of bistable systems are sensitive to a wide range of excitation frequencies, and notably sensitive in the extremely low frequency bandwidth. The low frequency range is particularly challenging for a linear resonant system to exploit due to stroke motion constraints that can inhibit the practicality of employing a resonant harvester.

The research and development interest in bistable energy harvester architectures and their appropriate dynamical implementation has consequently flourished [5,6]. By strategically exploiting the activation of snap-through dynamics, large energy conversion is realized. The motivation to harness the dynamics of bistable energy harvesting systems is grounded upon the pursuit of greater performance via larger amplitude snap-through dynamics as well as the practical realization that robust solutions are necessary to see the energy harvesting vision to success.

Typically, the objective is to activate continuous or repeated snap-through dynamics in the bistable harvester platform. However, for very low frequencies, the design of a bistable structure sensitive to such frequency spectra is a challenging endeavor. As a result, an alternative idea is considered, whereby occasional snap-through behaviors are exploited. The concept is often termed frequency up-conversion [5,50], in other words utilizing the very low frequency inputs to activate a state change in the bistable harvester that leads to a "ring down" intrawell oscillation. The ring down dynamics are partially dissipated via the electromechanical conversion, which provides a novel power generation strategy for extremely low frequency input vibrations. Thus, whether continuously or intermittently activated, the utilization of snap-through dynamics is a widely explored strategy to harness periodic input vibrations for energy harvesting aims.

On the other hand, not all ambient vibration resources are periodic. In fact, structural vibrations such as bridge/walkway oscillations due to vehicle or human motions are very often stochastic [51,52], and ocean wave heaves, which typically have a predominant spectral peak when evaluated over a given time period, have a large spread of the vibrational energy around the frequency of greatest energy concentration [47]. As a result, studies take care to investigate the stochastic excitation performance of energy harvesters [53]. In this context, bistable systems have unique advantages over alternative energy harvesting platforms when excited by noise. Whether by the stochastic resonance phenomenon using combined noise and periodic excitations or due only to stochastic inputs, an intelligent and effective design of the bistable harvester may activate the favorable snap-through dynamics when the stochastic inputs are otherwise insufficient to

greatly excite alternative architectures. The performance advantages of bistable vibration energy harvesters in stochastic excitation environments have been demonstrated for various stochastic spectra: including white Gaussian [54,55], exponentially-correlated [4], and band-limited [56] noises.

On the whole, the capacity to exploit a sensitive and robust array of energetic snap-through dynamics makes bistable energy harvester platforms effective candidates in the ever-growing exploration of novel means to transform the ambient vibrations around us into sustainable electrical energy resources.

### 1.3.3   Sensing and Detection

There are historic needs to monitor the changing dynamic responses of structures due to variation in the applied loads or the internal composition of the monitored system itself. The needs are numerous and the engineering and scientific applications of sensing structural changes are found on an enormous extent of length scales. Some examples of current research and industrial interest include the detection of miniscule force or mass change on micro- or nanoscale resonators [57], the health condition monitoring of commercial aircraft before, during, and after flights [58], and tracking the long-term wear-and-tear on massive civil infrastructure systems such as bridges [59]. By employing sensors to detect parameter shifts in the observed dynamic responses, the safety, performance, and longevity of numerous structural systems are ensured, which has broad and positive impact on society.

Sensitivity and accuracy are two critical objectives in detection methodologies. How these aims are achieved depends upon the length scale of interest as well as the detection approach which is employed. Vibration-based sensing strategies are commonly used due to an ease of implementation and ability to monitor global features of a structure. Across scales, a conventional implementation of vibration-based sensing is to track shifts in important structural frequency response data. For example, in microscale sensing of gaseous or chemical mass (like hazardous materials or fumes), the primary structural responses to observe are the changing resonant characteristics of the sensor due to the adsorbing mass on the sensor surface. Thus, the resonant frequency or phase shift at resonance is tracked over time and translated through a sensor model to the adsorbed quantity of mass [60]. The same overall detection strategy is used in meso-/macro-scale vibration-based sensing with frequency shifts, although on such scales the shifting dynamic characteristics might be attributed to damage features [58].

A serious difficulty for the otherwise favorable frequency shift-based detection strategies is an inherent limitation in the confident quantification of small shifts in resonance frequency or phase due to structural variation. The difficulty becomes exaggerated when the sensor readout (or structural response) is corrupted by the influences of environmental or sensor noise and system damping. Such concerns challenge the accuracy of detection for all scales of application. Consequently, to overcome the obstacles to accuracy and robustness, an alternative, emerging vibration-based detection strategy has been explored based upon the activation of bifurcations in the response of strongly nonlinear sensors [61–63].

For clarity, representative bifurcations of a bistable system are illustrated in the analytical response prediction plots in Section 1.2. For example, in Figure 1.6a it is seen that a steady-state, low amplitude intrawell dynamic response of a bistable structure will be destabilized if the excitation frequency exceeds a critical value of $\omega \approx 1.08$; at such a time, the bistable system behaviors would suddenly transition to the high amplitude intrawell dynamic. In the context of sensing and detection, the onset of the bifurcation is translated through a sensor model back to the near-infinitesimal structural change which induced the large response amplitude jump. Thus, the limits of parameter shift detection in an ideal bifurcation-based method approach the observation of quantum events [64,65]. This ability sharply contrasts the far more constrained sensitivity bounds imposed on traditional frequency shift-based approaches due to the smallest increment of change that can be resolved in the monitored analog signal based on hardware performance.

Bifurcation-based sensing methods have recently been successfully applied to the microscale, where the nonlinearity required to undergo bifurcations is easily effected, whether by the application of particular excitations or due to the typical, forced oscillation amplitude of the sensors with respect to resting geometry [66,18]. From these studies, evidence of considerable robustness to noise and damping in the proposed sensing strategy has been demonstrated [67,68], which contrasts the limitations encountered by employing the traditional approach of tracking linear resonance features for microscale mass sensing. The underlying requirements in bifurcation-based detection strategies are the exploitation of strong nonlinearity in the sensor/structure and an intelligent methodology to activate a bifurcation in such a way as to denote change in the parameter one wishes to monitor. Bistable sensor platforms thoroughly meet these needs and indeed are introducing opportunities to extend bifurcation-based sensing to new applications beyond the microscale.

Bistable structures have distinct advantages in their exploitation as strongly nonlinear sensor platforms, such as a greater number of bifurcations to exploit due to the unique dynamical forms represented by the intra- and interwell oscillations; a dramatic difference in dynamic response levels may be induced which provides more apparent indicators of change following the bifurcation event; a wide variety of all-mechanical design compositions that could be employed, like pre-curved beams [69], to empower sensing operation free of constant active load requirements to maintain bistability; and bistable sensors may undergo static stable state transitions, for example to enable means for passive detection of thresholds like impact or acceleration events [70]. Thus, bistable sensor architectures are strong candidates in the development and implementation of bifurcation-based detection strategies by the combined exploitation of the energetic behaviors of snap-through and the selective (in other words, adaptable) activation of bifurcations from one dynamic or static state/regime to another.

The ease with which strong nonlinearity is realized makes the microscale a favorable domain to develop and explore bifurcation-based sensing systems and methods to greatly advance detection capabilities beyond traditional frequency shift-based strategies. Yet, there are numerous important sensing and monitoring interests on the macroscale that also suffer from the drawbacks of traditional

frequency shift-based sensing approaches. Unfortunately, most macroscale structures do not exhibit strong nonlinearity under ordinary operations, indicating a critical constituent of bifurcation-based sensing is often absent in the inherent structural systems. Recently, to surmount this concern, researchers have explored the integration of bistable electric circuitry with a piezoelectric transducer and the host, monitored structure which is facilitated by a transducer; one such integrated system schematic is shown in Figure 1.3d [11]. Using this architecture, a strong nonlinearity – bistability – is introduced into the structural-electrical system, and is specifically contained only within the circuit due to the one-way current flow provided by the circuit design. The monitoring system is thus capable of harnessing many of the benefits of a bistable sensor for bifurcation-based sensing, and the robustness of detection accuracy to adverse noise and damping is found to be achieved for macroscale structural monitoring [71]. By the strategic exploitation of a bistable circuitry and structural integration, the advantages of bifurcation-based sensing are able to be leveraged on the macroscale. Thus, the energetic responses and dynamic adaptability of bistable sensors helps to justify their recent popular exploration in many sensing applications and research areas [11,72,73].

The deliberate activation of the distinct dynamic responses of bistable sensors finds another useful implementation in the development of microscale electromechanical signal filters or detectors [74]. The overall concept of electromechanical signal filtering is to exploit frequency-dependent response characteristics to induce strongly variable response amplitudes or spectral concentrations in the oscillator dynamics so as to detect or pass certain input frequencies or convert the input frequency to another value [66]. On small scales, all-electrical signal filters are prone to high damping and it has been shown that electromechanical counterparts may empower substantially sharper passbands and cut-off rates for accurate and precise filtering performance. When strongly nonlinear microscale oscillators are employed, their implementation may be as straightforward as the activation of a bifurcation in the sensor response from a low (or no) amplitude oscillation to one of significantly greater amplitude [75], which can be engineered to effect a signal filtering influence due to the on/off-type of dynamic variation. More intricate filtering concepts have been investigated to exploit multiharmonic behaviors in the microscale devices, such as the inducement of additional harmonics to leverage a greater versatility in filtering capability using an individual device architecture [76].

Due to the wide variety of behaviors that may be exploited and the dramatic difference in response amplitude between dynamic regimes for sharp filtering features, the dynamics of bistable oscillators indicate such microscale systems are strong candidates in the development of effective and adaptable filtering platforms [7]. For instance, Figure 1.12 exemplifies the versatility of bistable systems via multiharmonic behaviors produced in consequence to a single frequency of excitation: a frequency $\omega$ is input into the system but induces dynamics primarily at $\omega/3$ or $2\omega$. As a result, a microscale bistable oscillator can be harnessed to monitor particular harmonics of a given input frequency, minimizing the number of filters needed to be employed in series to achieve the same task. Thus, whether used for direct frequency bandpass filtering via the activation of low-to-high

response amplitude bifurcations or for the versatile harmonic response modulation features, bistable systems present new opportunities for electromechanical signal filtering and detection. The recent studies exploring such potential suggest there is much left to be uncovered and leveraged [7,70].

## 1.4 Outline of This Book

In summary, bistable systems can be realized using numerous methods, and the architecture that is selected for an application depends strongly on how it will be leveraged, whether the aims are to control vibration or convert vibrational energies to electrical power or to detect infinitesimal mass particles upon a micromechanical sensor. Although a variety of characteristics make the dynamics of bistable structures unique, the highly energetic behaviors and the ability to intelligently adapt dynamics for specific operational purposes are common rationales for the exploitation of bistable systems. Following this introductory assessment of the features of bistable structural dynamics that make them attractive for a variety of scientific and engineering purposes, the remainder of this book details the recent research achievements that have been made via strategically harnessing the dynamics of bistable systems, specifically within the fields of (i) vibration control; (ii) vibration energy harvesting; and, (iii) sensing and detection.

Prior to elaborating on the state of the art in these areas, Chapter 2 provides an overview of the theoretical foundations which are central to the modeling and analysis of bistable structural responses. The theoretical developments are provided in such a way as to allow readers with sufficient knowledge of vibrations and structural dynamics an accessible introduction to the common approaches which are used to mathematically investigate the strongly nonlinear dynamics of bistable systems. Readers with more advanced theoretical backgrounds may wish to continue directly to the subsequent chapters which contain more detailed mathematical developments specific to the bistable system architectures considered therein.

Chapter 3 describes how researchers are discovering new and high performance means for vibration damping, isolation, and absorption by exploiting the distinct, energetic dynamics of bistable structures. Concepts such as bistable isolators, snap-through absorbers, and adaptive damping elements are detailed from their modeling formulations and treatments through their experimental investigations, showing that effective performance relies on a knowledgeable design and utilization of bistability. Recent explorations of multi-body vibration control architectures are presented, indicating that harnessing the energetic and adaptable behaviors of bistable devices within system architectures can lead to enhanced performance when they are appropriately leveraged.

Chapter 4 describes the popular and successful implementation of bistable dynamics in vibration energy harvesting systems to enable exceptional and robust performance when excited by a variety of ambient vibration sources. The chapter details how researchers are using rigorous mathematical frameworks supplemented with careful laboratory and field examinations to derive generalized

insight into the effective exploitation of snap-through dynamics for high and consistent energy harvesting performance. Analytical and experimental developments are presented which clearly show that single and multiple DOF architectures may intelligently harness the energetic dynamics of bistable structures to broadly advance the aims of vibration-based energy harvesting.

Chapter 5 discusses how the adaptive and energetic dynamics of bistable structures have been exploited for the sensing and detection of changing system characteristics. Through research efforts that represent a large range of length scales and sensing applications, it is shown that intelligently leveraged transitions from one dynamic regime to another provide bistable sensor architectures with a detection capacity that is particularly sensitive and versatile. The chapter details analytical and experimental studies that investigate new bifurcation-based sensing strategies which find that the dynamics of bistable sensors may be effectively harnessed for high robustness to inevitable noise and damping influences.

To conclude, Chapter 6 surveys the emerging areas and outstanding issues that remain to be addressed in order to realize the greatest benefits for the three technical fields of interest here via harnessing the dynamics of bistable structures. The issues are described in terms of analytical understanding of the effective strategies for leveraging the dynamical behaviors as well as practical matters involved in the design, fabrication, experimentation, and deployment of bistable systems. Looking further forward, the book closes with a prospective summary of research avenues which may yet emerge, and discusses how the future ventures may be beneficially grounded via the state-of-the-art development and exploitation of bistable structural dynamics.

## References

[1] K. Yang, R.L. Harne, K.W. Wang, *et al.*, Dynamic stabilization of a bistable suspension system attached to a flexible host structure for operational safety enhancement, *Journal of Sound and Vibration* **333**, 6651–6661 (2014).

[2] A.F. Arrieta, P. Hagedorn, A. Erturk, *et al.*, A piezoelectric bistable plate for nonlinear broadband energy harvesting, *Applied Physics Letters* **97**, 104102 (2010).

[3] D.N. Betts, H.A. Kim, C.R. Bowen, Modeling and optimization of bistable composite laminates for piezoelectric actuation, *Journal of Intelligent Material Systems and Structures* **22**, 2181–2191 (2011).

[4] R.L. Harne, K.W. Wang, Prospects for nonlinear energy harvesting systems designed near the elastic stability limit when driven by colored noise, *ASME Journal of Vibration and Acoustics* **136**, 021009 (2014).

[5] R.L. Harne, K.W. Wang, A review of the recent research on vibration energy harvesting via bistable systems, *Smart Materials and Structures* **22**, 023001 (2013).

[6] S.P. Pellegrini, N. Tolou, M. Schenk, *et al.*, Bistable vibration energy harvesters: a review, *Journal of Intelligent Material Systems and Structures* **24**, 1303–1312 (2013).

[7] H.M. Ouakad, M.I. Younis, On using the dynamic snap-through motion of MEMS initially curved microbeams for filtering applications, *Journal of Sound and Vibration* **333**, 555–568 (2014).

[8] M. Bagheri, M. Poot, L. Mo, *et al.*, Dynamic manipulation of nanomechanical resonators in the high-amplitude regime and non-volatile mechanical memory operation, *Nature Nanotechnology* **6**, 726–732 (2011).

[9] M.T.A. Saif, On a tunable bistable MEMS – theory and experiment, *Journal of Microelectromechanical Systems* **9**, 157–170 (2000).

[10] S. Krylov, B.R. Ilic, D. Schreiber, *et al.*, The pull-in behavior of electrostatically actuated bistable microstructures, *Journal of Micromechanics and Microengineering* **18**, 055026 (2008).

[11] R.L. Harne, K.W. Wang, Robust sensing methodology for detecting change with bistable circuitry dynamics tailoring, *Applied Physics Letters* **102**, 203506 (2013).

[12] F. Moss, P.V.E. McClintock, eds, *Noise in Nonlinear Dynamical Systems, Volume 3: Experiments and Simulations* (Cambridge University Press, Cambridge, 1989).

[13] S.P. Timoshenko, *Theory of Elastic Stability* (McGraw-Hill, New York, 1936).

[14] I. Kovacic, M.J. Brennan, eds, *The Duffing Equation: Nonlinear Oscillators and their Behaviour* 1st edn (John Wiley & Sons, Ltd, Chichester, 2011).

[15] R. Seydel, *Practical Bifurcation and Stability Analysis* (Springer, New York, 2010).

[16] Y.A. Kuznetsov, *Elements of Applied Bifurcation Theory* (Springer, New York, 1998).

[17] M.I. Younis, *MEMS Linear and Nonlinear Statics and Dynamics* (Springer, New York, 2011).

[18] R. Lifshitz, M.C. Cross. *Nonlinear Dynamics of Nanomechanical and Micromechanical Resonators.* In H.G. Schuster, ed. *Reviews of Nonlinear Dynamics and Complexity: Volume 1* (Wiley-VCH Verlag GmbH, Weinheim 2008) pp. 1–52.

[19] F.C. Moon, *Chaotic and Fractal Dynamics : an Introduction for Applied Scientists and Engineers* (John Wiley & Sons, Inc., New York, 1992).

[20] S.H. Strogatz, *Nonlinear Dynamics and Chaos: with Applications to Physics, Biology, Chemistry, and Engineering* (Addison-Wesley, Reading, Massachusetts, 1994).

[21] P. Glendinning, *Stability, Instability and Chaos: an Introduction to the Theory of Nonlinear Differential Equations* (Cambridge University Press, Cambridge, 1994).

[22] J. Gleick, *Chaos* (Viking, New York, 1987).

[23] E. Lorenz, *The Essence of Chaos* (CRC Press, Florence, Kentucky, 1995).

[24] L. Gammaitoni, P. Hänggi, P. Jung, *et al.*, Stochasic resonance, *Reviews of Modern Physics* **70**(1), 223–287 (1998).

[25] T. Wellens, V. Shatokhin, A. Buchleitner, Stochastic resonance, *Reports on Progress in Physics* **67**, 45–105 (2004).

[26] S. Piggott, *The Earliest Wheeled Transport: From the Atlantic Coast to the Caspian Sea* (Cornell University Press, Ithaca, NY, 1983).

[27] H. Frahm. Means for damping the rolling motion of ships. U.S. Patent 970,368. U.S. Patent Office; 1910.

[28] D.P. Taylor, 1996 Fluid dampers for applications of seismic energy dissipation and seismic isolation. In *Proceedings of the Eleventh World Conference on Earthquake Engineering*; Acapulco, Mexico.

**[29]** B.B. Holmes. Shock absorber. U.S. Patent 1,751,479. United States Patent Office; 1930.

**[30]** D.J. Wagg, L.N. Virgin, *Exploiting Nonlinear Behavior in Structural Dynamics* (Springer, New York, 2012).

**[31]** A.F. Vakakis, O.V. Gendelman, L.A. Bergman, *et al*., *Nonlinear Targeted Energy Transfer in Mechanical and Structural Systems* (Springer, Dordrecht, 2008).

**[32]** R.S. Lakes, Extreme damping in composite materials with a negative stiffness phase, *Physical Review Letters* **86**, 2897–2900 (2001).

**[33]** M.E. Pontecorvo, S. Barbarino, F.S. Gandhi, *et al*., 2013 A load-bearing structural element with energy dissipation capability under harmonic excitation. In *Proceedings of the ASME 2013 Conference on Smart Materials, Adaptive Structures and Intelligent Systems*; Snowbird, Utah, USA. SMASIS2013-3060.

**[34]** D.R. Johnson, M. Thota, F. Semperlotti, *et al*., On achieving high and adaptable damping via a bistable oscillator, *Smart Materials and Structures* **22**, 115027 (2013).

**[35]** G.J. Murray, F. Gandhi, 2011 The use of damping to mitigate violent snap-through of bistable systems. In *Proceedings of the ASME 2011 Conference on Smart Materials, Adaptive Structures and Intelligent Systems SMASIS2011*; Scottsdale, Arizona. SMASIS2011-4997.

**[36]** R. Wiebe, L.N. Virgin, I. Stanciulescu, *et al*., Characterizing dynamic transitions associated with snap-through: a discrete system, *Journal of Computational and Nonlinear Dynamics* **8**, 011010 (2013).

**[37]** J. Winterflood, T. Barber, D.G. Blair, Using Euler buckling springs for vibration isolation, *Classical and Quantum Gravity* **19**, 1639–1645 (2002).

**[38]** L.N. Virgin, R.B. Davis, Vibration isolation using buckled struts, *Journal of Sound and Vibration* **260**, 965–973 (2003).

**[39]** D.T.R. Pasala, A.A. Sarlis, S. Nagarajaiah, *et al*., Adaptive negative stiffness: new structural modification approach for seismic protection, *Journal of Structural Engineering* **139**, 1112–1123 (2013).

**[40]** A. Sarlis, D. Pasala, M. Constantinou, *et al*., Negative stiffness device for seismic protection of structures, *Journal of Structural Engineering* **139**, 1124–1133 (2013).

**[41]** O.V. Gendelman, C.H. Lamarque, Dynamics of linear oscillator coupled to strongly nonlinear attachment with multiple states of equilibrium, *Chaos, Solitons and Fractals* **24**, 501–509 (2005).

**[42]** D.R. Johnson, R.L. Harne, K.W. Wang, A disturbance cancellation perspective on vibration control using a bistable snap-through attachment, *Journal of Vibration and Acoustics* **136**, 031006 (2014).

**[43]** L.I. Manevitch, G. Sigalov, F. Romeo, *et al*., Dynamics of a linear oscillator coupled to a bistable light attachment: analytical study, *Journal of Applied Mechanics* **81**, 041011 (2014).

**[44]** S. Priya, D.J. Inman, *Energy Harvesting Technologies* (Springer, New York, 2009).

**[45]** A. Erturk, D.J. Inman, *Piezoelectric Energy Harvesting* (John Wiley & Sons, Ltd, Chichester, 2011).

**[46]** N. Elvin, A. Erturk, *Advances in Energy Harvesting Methods* (Springer, New York, 2013).

**[47]** J. Cruz, *Ocean Wave Energy: Current Status and Future Perspectives* (Springer, Berlin, 2008).

**[48]** J. Scruggs, P. Jacob, Harvesting ocean wave energy, *Science* **323**, 1176–1178 (2009).

**[49]** L. Zuo, X. Tang, Large-scale vibration energy harvesting, *Journal of Intelligent Material Systems and Structures* **24**, 1405–1430 (2013).

**[50]** L. Tang, Y. Yang, C.K. Soh, Toward broadband vibration-based energy harvesting, *Journal of Intelligent Material Systems and Structures* **21**, 1867–1897 (2010).

**[51]** Z. Li, L. Zuo, J. Kuang, G. Luhrs, Energy-harvesting shock absorber with a mechanical motion rectifier, *Smart Materials and Structures* **22**, 025008 (2013).

**[52]** P.L. Green, E. Papatheou, N.D. Sims, Energy harvesting from human motion and bridge vibrations: an evaluation of current nonlinear energy harvesting solutions, *Journal of Intelligent Material Systems and Structures* **24**, 1494–1505 (2013).

**[53]** M.F. Daqaq, R. Masana, A. Erturk, D.D. Quinn, On the role of nonlinearities in vibratory energy harvesting: a critical review and discussion, *Applied Mechanics Reviews* **66**, 040801 (2014).

**[54]** C.R. McInnes, D.G. Gorman, M.P. Cartmell, Enhanced vibrational energy harvesting using nonlinear stochastic resonance, *Journal of Sound and Vibration* **318**, 655–662 (2008).

**[55]** S. Zhao, A. Erturk, On the stochastic excitation of monostable and bistable electroelastic power generators: relative advantages and tradeoffs in a physical system, *Applied Physics Letters* **102**, 103902 (2013).

**[56]** R. Masana, M.F. Daqaq, Response of Duffing-type harvesters to band-limited noise, *Journal of Sound and Vibrations* **332**, 67556767 (2013).

**[57]** J.W. Gardner, V.K. Varadan, O.O. Awadelkarim, *Microsensors, MEMS, and Smart Devices* (John Wiley & Sons, Ltd, Chichester, 2001).

**[58]** F.K. Chang, *Structural Health Monitoring* (Technomic, Lancaster, Pennsylvania, 1999).

**[59]** F. Ansari, *Sensing Issues in Civil Structural Health Monitoring* (Springer, Dordrecht, The Netherlands, 2005).

**[60]** T. Thundat, E.A. Wachter, S.L. Sharp, R.J. Warmack, Detection of mercury vapor using resonating microcantilevers, *Applied Physics Letters* **66**, 1695–1697 (1995).

**[61]** W. Zhang, K.L. Turner, 2004 A mass sensor based on parametric resonance. In *Proceedings of Solid-State Sensor, Actuator and Microsystems Workshop*; Hilton Head Island, South Carolina. 49–52.

**[62]** M.I. Younis, F. Alsaleem, Exploration of new concepts for mass detection in electrostatically-actuated structures based on nonlinear phenomena, *Journal of Computational and Nonlinear Dynamics* **4**, 021010 (2009).

**[63]** V. Kumar, *et al.*, Bifurcation-based mass sensing using piezoelectrically-actuated microcantilevers, *Applied Physics Letters* **98**, 153510 (2011).

**[64]** A.B. Zorin, Quantum-limited electrometer based on single cooper pair tunneling, *Physical Review Letters* **76**, 4408–4411 (1996).

**[65]** R. Vijay, M.H. Devoret, I. Siddiqi, Invited review article: the Josephson bifurcation amplifier, *Review of Scientific Instruments* **80**, 111101 (2009).

**[66]** J.F. Rhoads, S.W. Shaw, K.L. Turner, Nonlinear dynamics and its applications in micro- and nanoresonators, *Journal of Dynamic Systems, Measurement, and Control* **132**, 034001 (2010).

**[67]** W. Zhang, K.L. Turner, Application of parametric resonance amplification in a single-crystal silicon micro-oscillator based mass sensor, *Sensors and Actuators A* **122**, 23–30 (2005).

**[68]** K.L. Turner, C. Burgner, Z. Yie, *et al.*, Nonlinear dynamics of MEMS systems, *AIP Conference Proceedings* **1339**, 111 (2011).

**[69]** J. Qiu, J.H. Lang, A.H. Slocum, A curved-beam bistable mechanism, *Journal of Microelectromechanical Systems* **13**, 137–146 (2004).

**[70]** H.M. Ouakad, M.I. Younis, The dynamic behavior of MEMS arch resonators actuated electrically, *International Journal of Non-Linear Mechanics* **45**, 704–713 (2010).

**[71]** J. Kim, R.L. Harne, K.W. Wang, Enhancing damage identification robustness to noise and damping using integrated bistable and adaptive piezoelectric circuitry, **137**, 011005 (2015).

**[72]** M.I. Younis, H.M. Ouakad, F.M. Alsaleem, R. Miles, W. Cui, Nonlinear dynamics of MEMS arches under harmonic electrostatic actuation, *Journal of Microelectromechanical Systems* **19**, 647–656 (2010).

**[73]** S. Krylov, B.R. Ilic, S. Lulinsky, Bistability of curved microbeams actuated by fringing electrostatic fields, *Nonlinear Dynamics* **66**, 403–426 (2011).

**[74]** F.D. Bannon, J.R. Clark, C.T.C. Nguyen, High-Q HF micromechanical filters, *IEEE Journal of Solid-State Circuits* **35**, 512–526 (2000).

**[75]** J.F. Rhoads, S.W. Shaw, K.L. Turner, Nonlinear response of resonant microbeam systems with purely-parametric electrostatic actuation, *Journal of Micromechanics and Microengineering* **16**, 890–899 (2006).

**[76]** B.K. Hammad, A.H. Nayfeh, E.M. Abdel-Rahman, On the use of the subharmonic resonance as a method for filtration, *Journal of Computational and Nonlinear Dynamics* **6**, 041007 (2011).